ARMY RESEARCH LABORATORY

Characterization of Jet Flow From a Decaying Wave Blast Simulator

Stephen J. Schraml

ARL-TR-1259

JANUARY 1997

DTIC QUALITY INSPECTED 4

19970203 039

Army Research Laboratory
Aberdeen Proving Ground, MD 21005-5425

ARL-TR-1259   January 1997

Characterization of Jet Flow From a Decaying Wave Blast Simulator

Stephen J. Schraml
Weapons & Materials Research Directorate

Abstract

A computational study was performed to characterize the time-dependent jet flow exiting the expansion tunnel of the large blast/thermal simulator (LB/TS). The aerodynamic environment produced by the jet flow has been identified as a possible means of testing full scale military equipment in high drag blast events. Two-dimensional (2-D) axisymmetric calculations were used to estimate the peak pressure, velocity, and impulse levels in the jet flow as a function of the initial conditions. Next, a set of 2-D planar symmetry calculations was performed to assess the effect of the ground plane on the flow field and determine the changes in flow parameters as a function of distance from the exit plane. Finally, a set of three-dimensional (3-D) calculations was used to generate a detailed description of the time-dependent flow and to determine its spatial uniformity for vehicle testing. The 3-D calculation simulating the maximum operational limit of the facility resulted in a peak flow velocity of approximately 420 m/s in an event with a duration of approximately 1.2 s.

ACKNOWLEDGMENTS

INTENTIONALLY LEFT BLANK

TABLE OF CONTENTS

INTENTIONALLY LEFT BLANK

LIST OF FIGURES

LIST OF FIGURES (continued)

1. INTRODUCTION

Many Army ground systems have designated criteria for survival in a nuclear blast environment. The survivability criteria for these systems are based on an assumption of *ideal*[1] blast: the propagation of the nuclear blast wave over a surface that is perfectly smooth, flat, and reflective of all thermal and mechanical energy. Conversely, significant modification of the blast wave by surface characteristics is referred to as *non-ideal*[1] blast.

When a nuclear weapon is detonated over land, the thermal radiation heats the ground and creates a stratified layer of air with a high sound speed. When the leading shock created by the blast reaches the high sound speed air, it is accelerated, resulting in a jet of high speed flow along the ground. This effect was first observed in nuclear weapons tests of the 1950s and 1960s, and its effect is illustrated in Figure 1. This figure compares the expected ideal static overpressure and dynamic pressure histories (dashed lines) to the observed non-ideal blast histories[2] (solid lines). The acceleration of the flow by the interaction with the high sound speed air causes the leading shock to be weakened as illustrated by the earlier arrival of a lower amplitude shock in the static overpressure chart. However, the most significant effect of the thermal modification of the blast wave can be seen in the dynamic pressure chart. In this type of event, the peak dynamic pressure can be much greater than that of the ideal case, and the dynamic pressure impulse (the area under the dynamic pressure curve) can be several times that of the ideal.
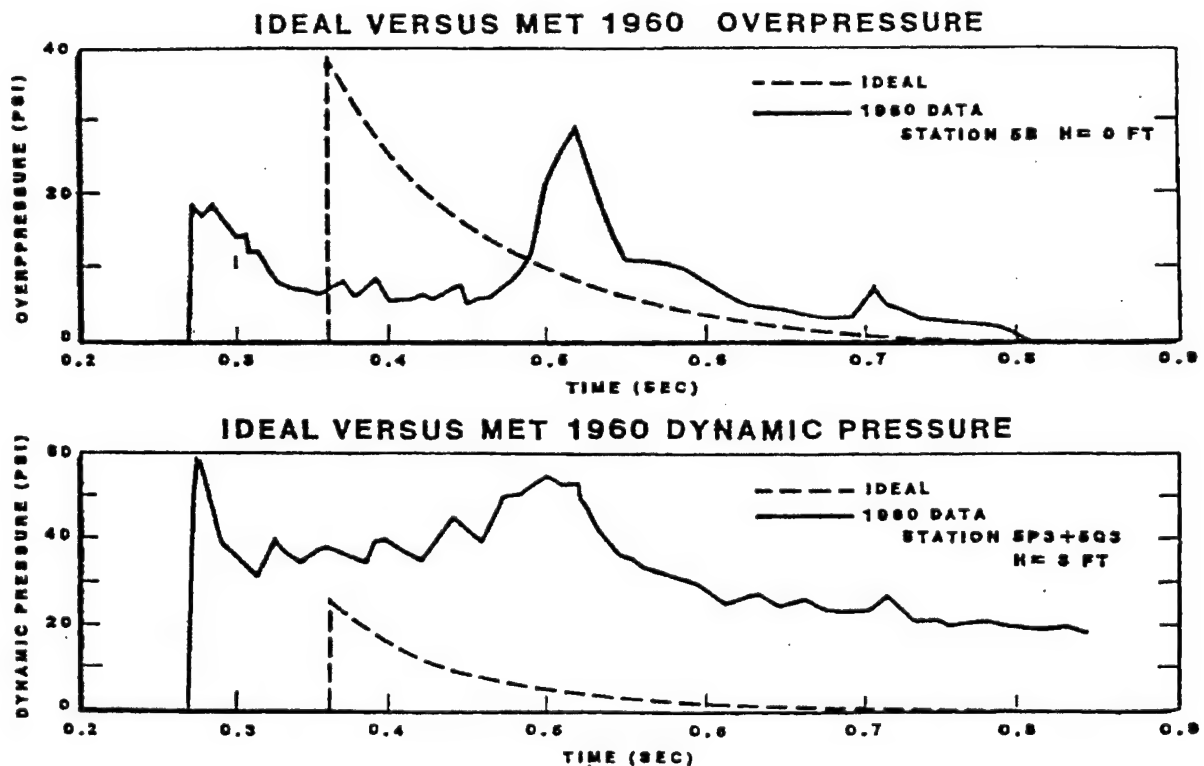

Figure 1. Comparison of Ideal and Non-Ideal Waveforms.

1

Dynamic pressure is defined as the kinetic energy per unit volume of a fluid in motion and is responsible for drag loading on objects subjected to blast flows. This drag loading typically results in the whole body displacement of the object. Structural damage to the object results from impacts of the object with the ground after being set into motion by the blast load. The significance of the non-ideal blast effect to Army ground systems is that the existing survivability criteria do not consider the enhanced drag loading associated with this phenomenon. Consequently, some Army ground systems may have a hidden vulnerability that is not addressed in the current war-fighting doctrine. The absence of this information from the doctrine could potentially result in unexpected casualties on the battlefield.

To incorporate the effects of the non-ideal blast phenomenon into the doctrine, it is necessary to determine the whole body response of Army systems to high drag blast events. The most reliable means of obtaining this information for existing systems on real surfaces is through full scale experimentation. The large blast/thermal simulator[3] (LB/TS), which is the only facility in the United States for testing full scale equipment in the blast and thermal radiation environments produced by nuclear weapons, is located at the White Sands Missile Range, New Mexico, and is operated by the Defense Special Weapons Agency (DSWA).

The LB/TS (shown in Figure 2) is the world's largest shock tube, consisting primarily of a driver system, an expansion tunnel, and an active rarefaction wave eliminator[4] (RWE). The driver system consists of nine steel cylinders, each 1.83 m in diameter with lengths ranging from 11 m to 29 m. At the downstream end of each cylinder is a converging nozzle that reduces the available flow diameter of each tube to 91 cm. The driver tubes can be seen near the lower right corner of Figure 2. The expansion tunnel is a horizontal half-cylinder with a cross-sectional area of 163 m^2 and length of 170 m. The RWE is located at the downstream end of the expansion section (near the upper left corner of Figure 2). This device is used to minimize disturbances in the expansion tunnel flow, which are generated when the blast flow exits the expansion tunnel.
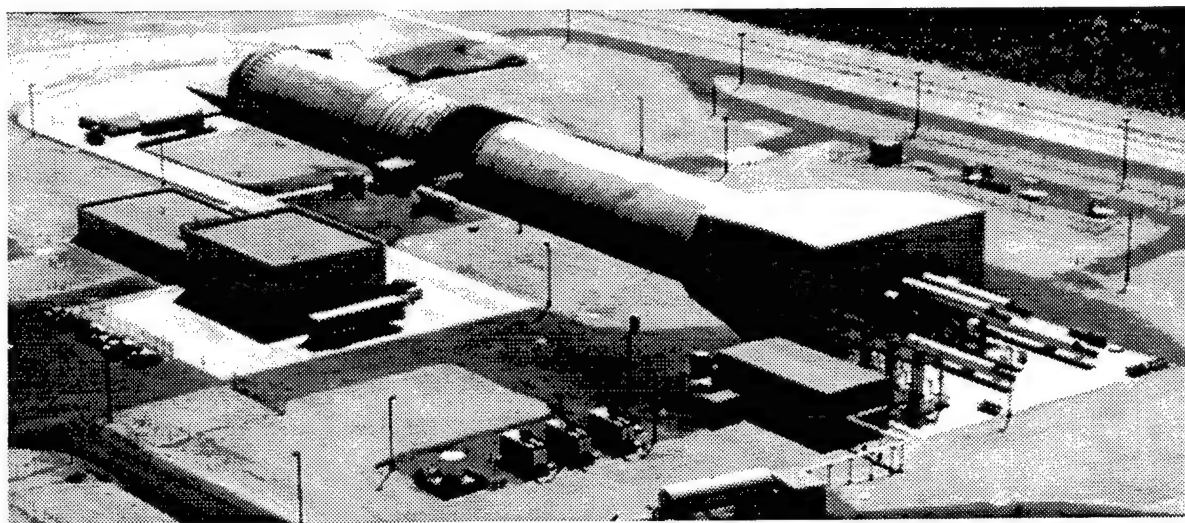

Figure 2. Large Blast/Thermal Simulator.

Blast waves are generated in the expansion tunnel of the LB/TS by first charging the driver tubes to high pressure with nitrogen gas. A steel diaphragm, located down stream from the converging nozzle, is used to contain the gas in each of the driver tubes. When the operational driver conditions are obtained, the nine diaphragms are simultaneously ruptured with an explosive charge, releasing the driver gas into the expansion section. The individual shocks from each driver tube expand into the tunnel and coalesce into a single planar shock. When the RWE is used, test articles placed inside the expansion tunnel are exposed to blast histories similar to the ideal curves illustrated in Figure 1.

The use of the LB/TS to generate non-ideal blast waveforms such as those illustrated in Figure 1 is outside the intended operation of that facility. Thus, to create these types of waveforms, alternate methods for operating the LB/TS had to be identified and explored. Work performed at the U.S. Army Research Laboratory (ARL) has demonstrated that the flow exiting the expansion section of a shock tube may be used to test full scale military equipment in the high drag flows associated with non-ideal blast.[5] This flow exiting the shock tube is referred to as the exit jet. When the leading shock is formed, it travels down the expansion tunnel, accelerating the initially ambient gas in the tunnel. Within the operational range of the LB/TS, the flow of the shocked air is subsonic. When this shock reaches the downstream end of the tunnel, it expands suddenly into the surrounding atmosphere. This sudden expansion causes a rarefaction wave to form which travels up stream into the expansion section, against the primary direction of flow. The pressure on the downstream side of the rarefaction wave is lower than that on the upstream side. Thus, the fluid initially accelerated by the primary shock is further accelerated when processed by the rarefaction wave. In LB/TS ideal blast operation, the purpose of the RWE is to eliminate the formation of this rarefaction wave. By removing the RWE from the expansion tunnel, the characteristics of the rarefaction wave may be exploited to produce the high velocity jet that is needed for non-ideal blast testing.

The use of the exit jet of the LB/TS represents a significant change in operation of that facility. Changes in facility configuration and operational procedure are costly and may not interfere with the ability of the facility to accomplish its original mission of simulating ideal blast events. Thus, it is important to estimate the performance of the facility under this new operational configuration. To accomplish this, a study was performed in which the LB/TS exit jet flow was simulated computationally. The computational study consisted of three distinct elements. First, a series of two-dimensional (2-D) axisymmetric calculations was performed to provide an initial indication of the changes in peak pressures, peak velocities, and energy delivery at various distances from the exit plane of the expansion tunnel as a function of initial driver gas conditions. Next, a set of 2-D planar symmetry calculations was performed to provide an initial indication of the effect of the ground plane on the primary shock. Finally, a three-dimensional (3-D) computational model was constructed and used to obtain a detailed description of the flow characteristics and complete the overall assessment of the exit jet as a technique for generating the desired transient flow environment.

2. AXISYMMETRIC CALCULATIONS

The initial phase of the computational study involved the use of a 2-D axisymmetric configuration to represent the LB/TS and the surrounding atmosphere. This configuration was the first to be used because axisymmetric models require a relatively small number of grid points to represent a particular geometry. Consequently, a set of axisymmetric calculations could be executed in a short period of time to determine the direction of the remainder of the study. However, the efficiency of the axisymmetric calculation comes at the expense of model fidelity. Specifically, the axisymmetric calculations do not represent the ground plane that exists down stream from the expansion tunnel exit. Because of this limitation, it was decided that the axisymmetric calculations would be used to qualitatively describe the overall blast wave shapes in the exit jet and estimate the dynamic pressure levels present in the exit jet as a function of initial driver gas overpressure. Since there is no representation of the ground plane in the axisymmetric configuration, the shock is allowed to expand spherically after it exits the expansion tunnel. This provides a lower bound on the incident static overpressure recorded at various distances from the tunnel exit. It can also be used as a means of validating computational results from models with greater fidelity with respect to the actual geometry. Since the axisymmetric calculations represent the lower bound on incident static overpressure, matching 3-D calculations should have greater incident static overpressures at the same locations.

The construction of the axisymmetric computational model is based on the preservation of relative lengths, areas, and volumes between the driver system, converging nozzle, and expansion tunnel of the subject geometry. For example, the driver system of the LB/TS consists of nine drivers, each with a converging nozzle at its downstream end. The axisymmetric representation of the LB/TS driver system consists of a single cylinder and converging nozzle with the identical cross-sectional area and volume as the nine LB/TS driver tubes. The expansion tunnel is represented by a cylinder with a diameter of 14.4 m to obtain the actual cross-sectional area of 163 m^2 in the semi-cylindrical expansion tunnel of the LB/TS. A schematic diagram illustrating the resulting axisymmetric model of the LB/TS is shown in Figure 3.

All 2-D calculations in the exit jet study were performed with the second order hydro-dynamic advanced research code[6] (SHARC), an explicit, finite difference[7], Euler[8] equation solver. The jet flow generated at the nozzle exit and the expansion tunnel exit is a source of shear flow. A k-ϵ[9] turbulence model was employed in the SHARC calculations to properly simulate the turbulent dissipation of kinetic energy created by the shear flow.

The first calculation in the study was configured to represent an initial driver gas over-pressure of 3.4 MPa and temperature of 288 K. Data-gathering stations placed in the computational domain were used to monitor the fluid properties as a function of time. These stations were located at various radii inside the expansion tunnel and down stream from the expansion tunnel. The stations in the tunnel were located 105 m from the upstream end of the expansion tunnel. This position corresponds to the location of test articles in ideal blast tests. Figures 4 and 5 plot the static overpressure and dynamic pressure, respectively, at this location for the 3.4-MPa case. These figures show the arrival of the leading shock at
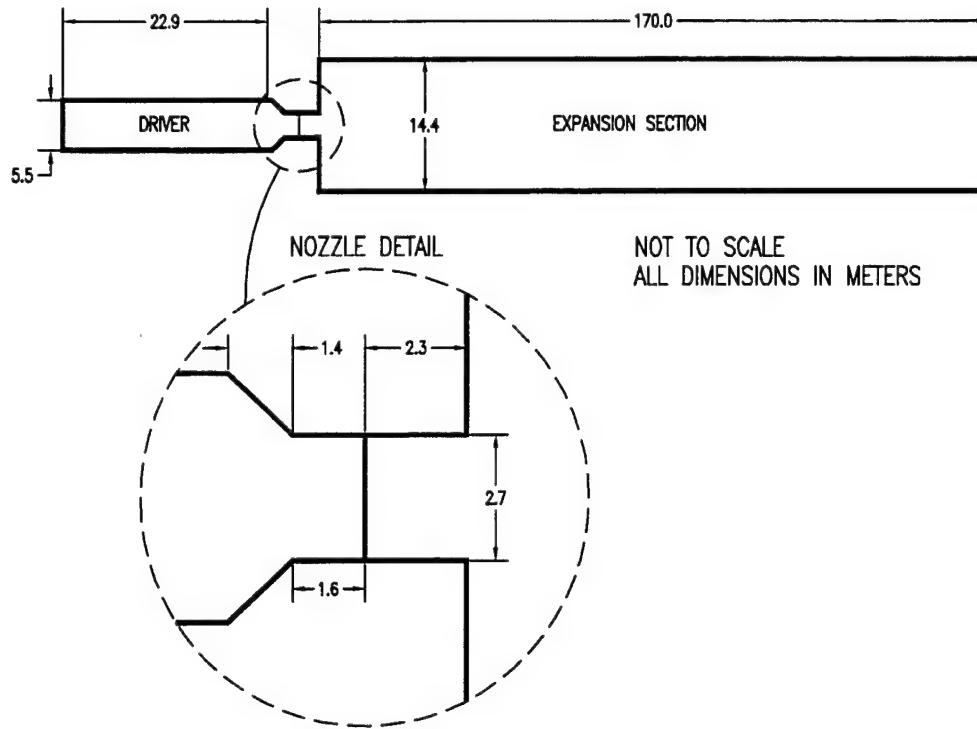
4

Figure 3. Axisymmetric Computational Model.

approximately 225 ms and having an incident static overpressure of approximately 85 kPa. A decay in the histories follows the incident shock until a time of approximately 600 ms, when the static overpressure suddenly decreases and drops below atmospheric pressure. At the same time, the dynamic pressure increases to reach a maximum of approximately 12 kPa at 950 ms. This drop in static overpressure and corresponding increase in dynamic pressure is a result of the rarefaction wave propagating up stream from the downstream end of the expansion section, accelerating the shocked gas. In cases when the RWE is used, this drop in static overpressure and increase in dynamic pressure are not present, and the resulting histories are representative of ideal blast waves.

The propagation of the rarefaction wave into the expansion tunnel converts internal energy into kinetic energy and provides the impetus for the formation of the exit jet. The velocity vector plot of Figure 6 corresponds to a time of 600 ms after flow initiation and shows the early formation of the jet as it exits the expansion tunnel. In this figure, the primary direction of flow is from the bottom of the figure to the top, and the downstream end of the expansion tunnel can be seen at the bottom of the figure ending at 170 m. This figure shows the jet as a coherent flow structure, retaining the shape of the expansion tunnel as it travels down stream. At the outer radius of the jet, the shear layer between the high speed jet and the ambient air forms a vortex ring identified by the circular pattern of velocity vectors.

Late in the event, the negative static overpressure inside the expansion tunnel creates an inflow of air into the tunnel to equilibrate with the ambient atmospheric pressure. In the velocity vector plot of Figure 7, corresponding to a time of 1.7 s after flow initiation, two

5
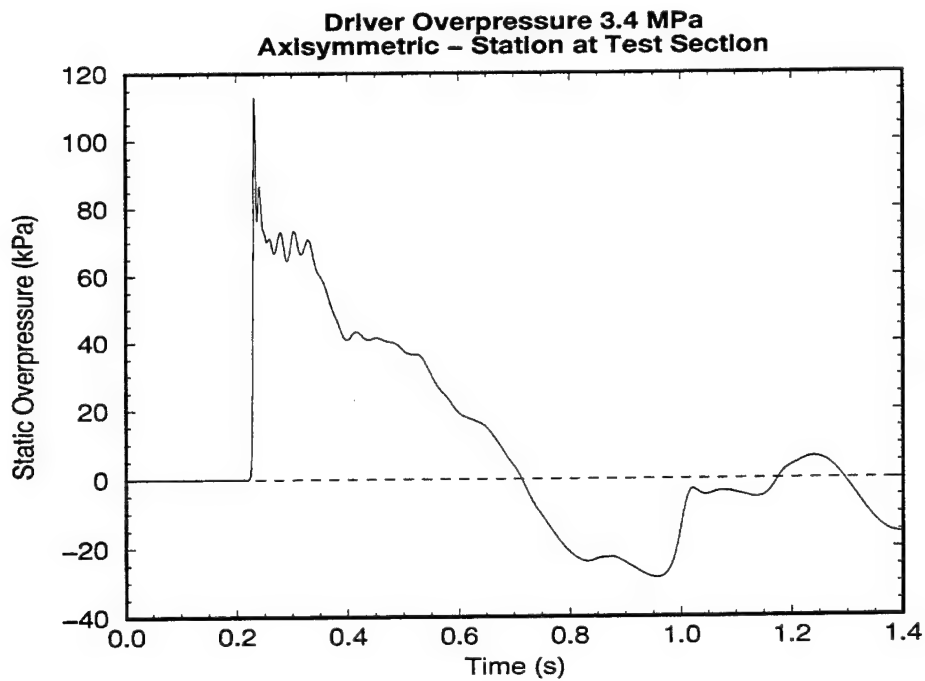
Figure 4. Axisymmetric Model: Static Overpressure in Expansion Tunnel.
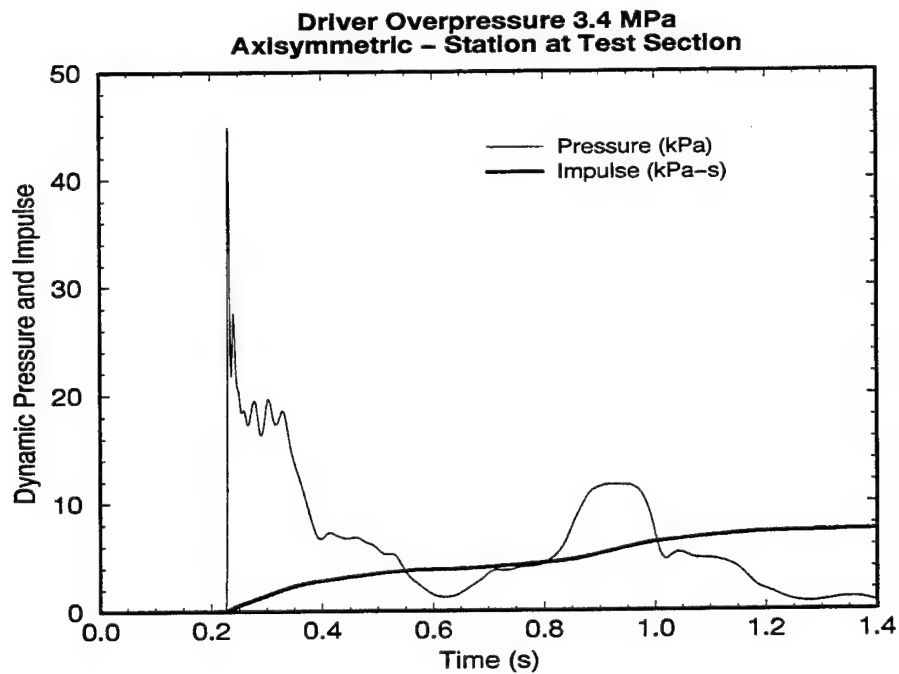
Figure 5. Axisymmetric Model: Dynamic Pressure in Expansion Tunnel.

6
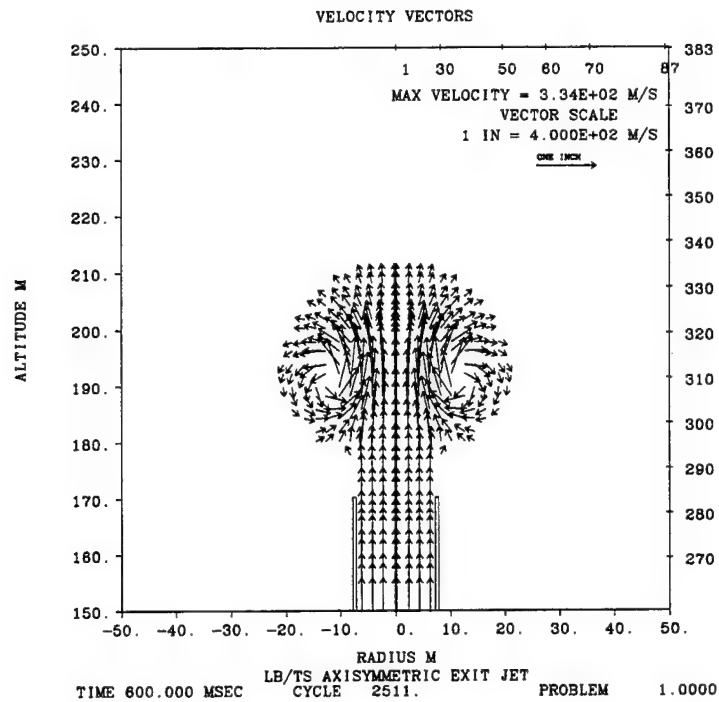
Figure 6. Axisymmetric Model: Velocity Vectors at 600 ms.
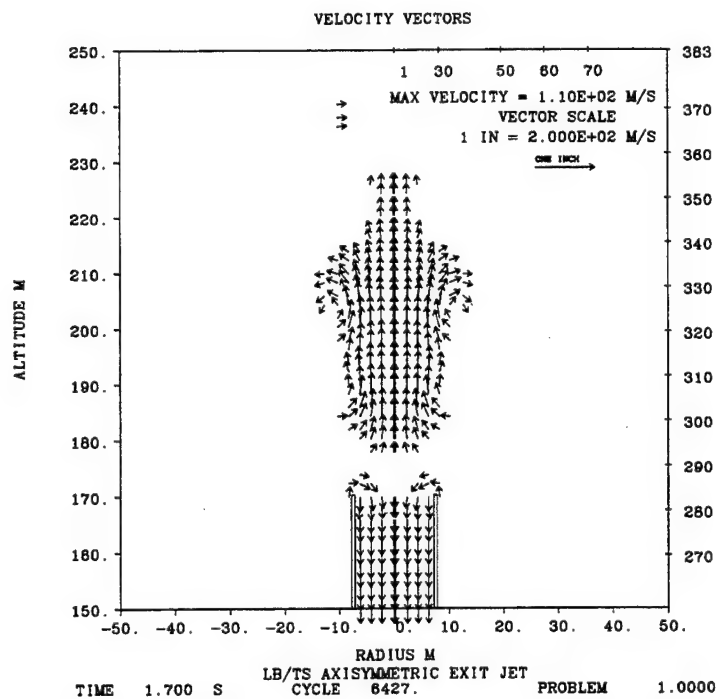
Figure 7. Axisymmetric Model: Velocity Vectors at 1.7 s.

Driver Overpressure 3.4 MPa
Axisymmetric – Station 40 m from Tunnel Exit

Figure 8. Axisymmetric Model: Static Overpressure in Exit Jet.

Driver Overpressure 3.4 MPa
Axisymmetric – Station 40 m from Tunnel Exit

Figure 9. Axisymmetric Model: Dynamic Pressure in Exit Jet.

8

Figure 10. Axisymmetric Model: Dynamic Pressure in Exit Jet.

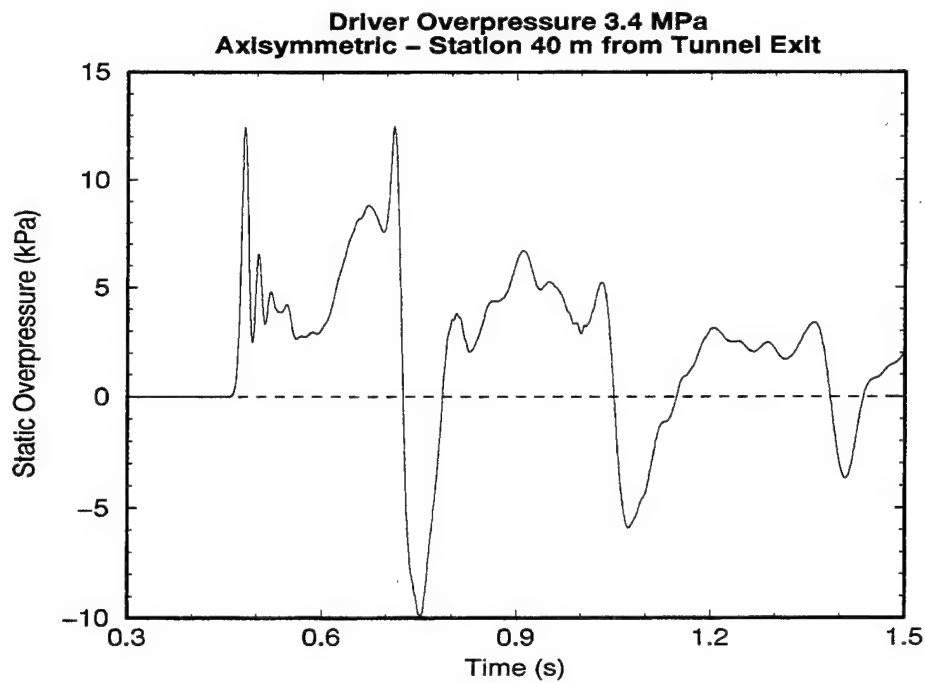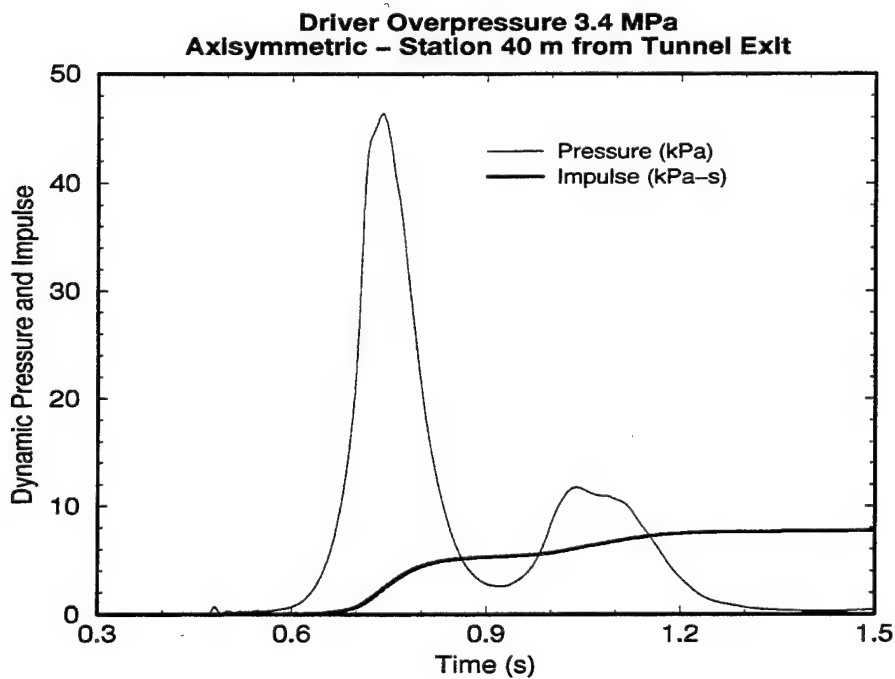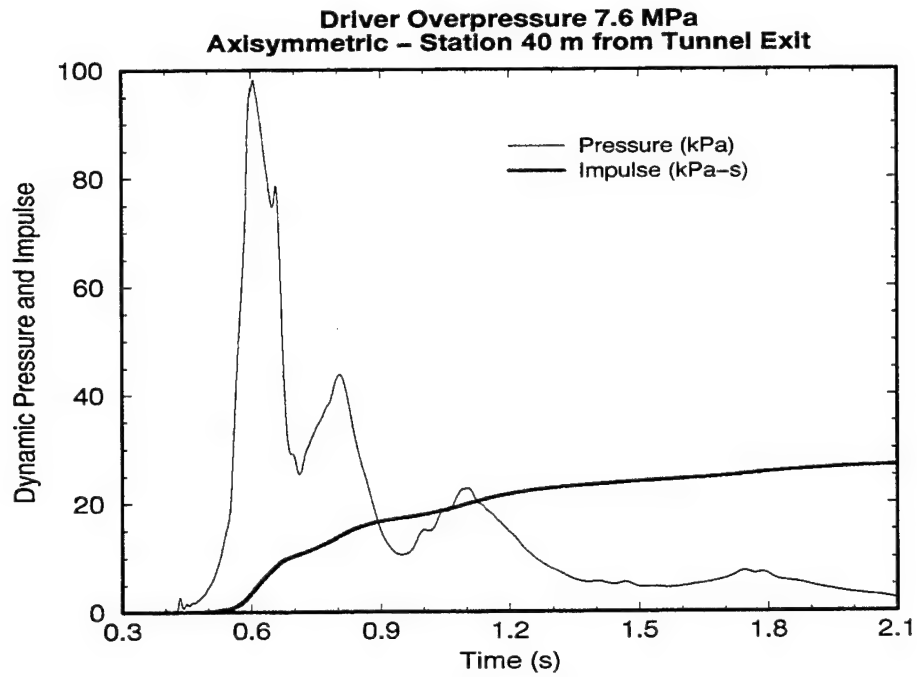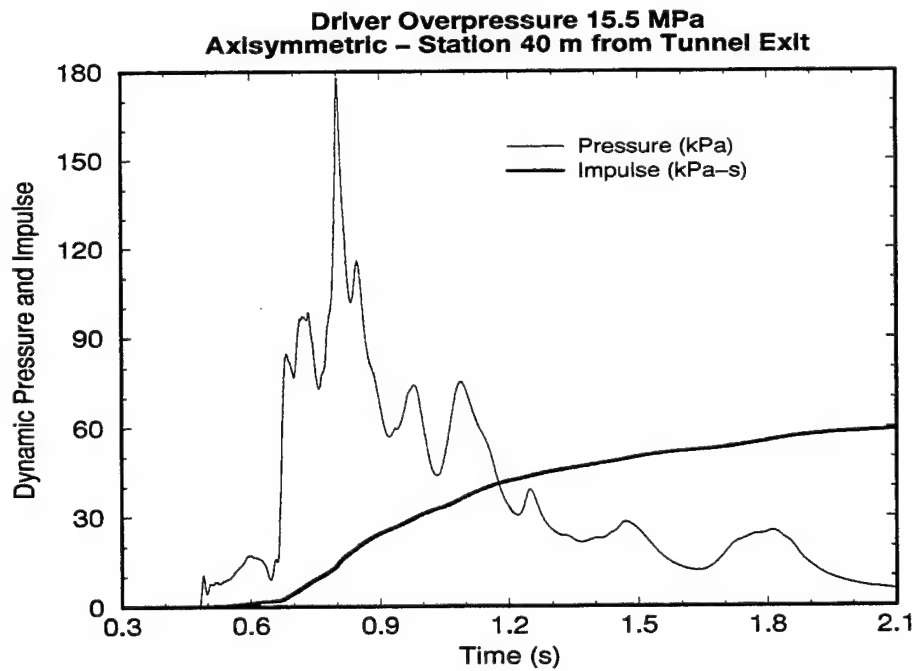Figure 11. Axisymmetric Model: Dynamic Pressure in Exit Jet.

9

distinct velocity patterns are visible: the core exit jet flow, traveling from bottom to top, and the inflow of air into the expansion tunnel created by the negative pressure phase in the tunnel. This figure provides an indication of the optimum location within the exit jet for testing of equipment. If the test article is placed too close to the exit plane of the expansion tunnel, its whole body response may be influenced by the negative flow direction during the inflow phase. If the target is placed too far from the tunnel, the full energy delivery potential of the exit jet may not be realized. From Figures 6 and 7, it is apparent that the best locations for equipment testing are in the range of 10 m to 40 m from the exit plane of the expansion tunnel.

The static overpressure recorded at a position 40 m down stream from the tunnel exit in the 3.4-MPa case is shown in Figure 8. At this location, the leading shock arrives at approximately 480 ms and has an initial amplitude of approximately 8 kPa. This incident overpressure is much less than that inside the tunnel and illustrates the decay of the static overpressure with increasing distance from the exit plane of the tunnel because of the spherical expansion of the shock into the surrounding atmosphere. After the arrival of the weak shock, the static overpressure history oscillates about ambient pressure.

The dynamic pressure history at this same location is provided in Figure 9 and is represented by the thin line in that chart. This curve shows the arrival of the weak shock as a small disturbance occuring at approximately 480 ms. The shocked expansion tunnel gas, accelerated by the formation of the rarefaction wave, reaches the measurement station at approximately 600 ms and causes the dynamic pressure to reach a maximum of 46 kPa at approximately 730 ms, followed by a decay to zero. The dynamic pressure impulse is represented in this figure with the thick line and shows the final dynamic pressure impulse to be 7.7 kPa-s.

Two additional axisymmetric calculations were performed to simulate initial driver overpressures of 7.6 MPa and 15.5 MPa (the maximum operational limit of the LB/TS). The dynamic pressure and impulse histories for these cases are provided in Figures 10 and 11 and exhibit the same wave pattern as the 3.4-MPa case. The peak dynamic pressures for these cases were 98 kPa and 178 kPa, respectively, while the final dynamic pressure impulses were 26.8 kPa-s for the 7.6-MPa case and 59.1 kPa-s for the 15.5-MPa case.

3. 2-D PLANAR SYMMETRY CALCULATIONS

With the axisymmetric calculations providing the initial estimate of the overall shape of the exit jet histories and dynamic pressure impulse levels that can be obtained from the exit jet, the next phase in the study was to estimate the effect of the ground plane on the expansion of the shock and the primary flow. A 2-D planar symmetry model was used for this part of the study. While the axisymmetric configuration treats the computational domain as a surface of revolution about the centerline, the 2-D planar configuration treats the computational domain as completely uniform in the direction normal to the domain. Thus, the computational domain is assumed to have a unit of uniform depth normal to the computational grid.

10

As described, the axisymmetric configuration allowed the leading shock to expand spherically down stream from the exit of the expansion tunnel. This resulted in a lower bound on the incident static overpressures that would be observed in the exit jet. Conversely, the planar symmetry model limits the expansion of the leading shock because of the presence of the ground plane and the assumption of uniformity in the plane normal to the computational domain. Thus, the planar symmetry configuration will limit the expansion of the leading shock and provide an upper bound on the amplitude of the incident shock at data-gathering stations down stream from the expansion section. These characteristics allow the incident static overpressure levels obtained from the two configurations to serve as upper and lower limits on the actual incident overpressures.

A schematic diagram of the 2-D planar symmetry computational model is provided in Figure 12. The diameter of the semi-cylindrical expansion section of the LB/TS is approximately 20 m. Accordingly, the development of the planar symmetry model is based on an assumed unit depth of 20 m. As a result, the height of the expansion tunnel in the planar model is 8.16 m to produce the cross-sectional area of 163 m^2 in the expansion section. Likewise, the areas of the driver tube and converging nozzle are also appropriately scaled on the 20-m unit depth assumption to preserve the area and volume relationships of the LB/TS. The floor of the expansion tunnel and the ground plane that lies down stream from the expansion tunnel are modeled by the flat, reflective bottom boundary of the computational domain. The actual ground plane down stream from the LB/TS expansion tunnel is not flat, but it was decided that modeling it as such would be sufficient for this exploratory study.

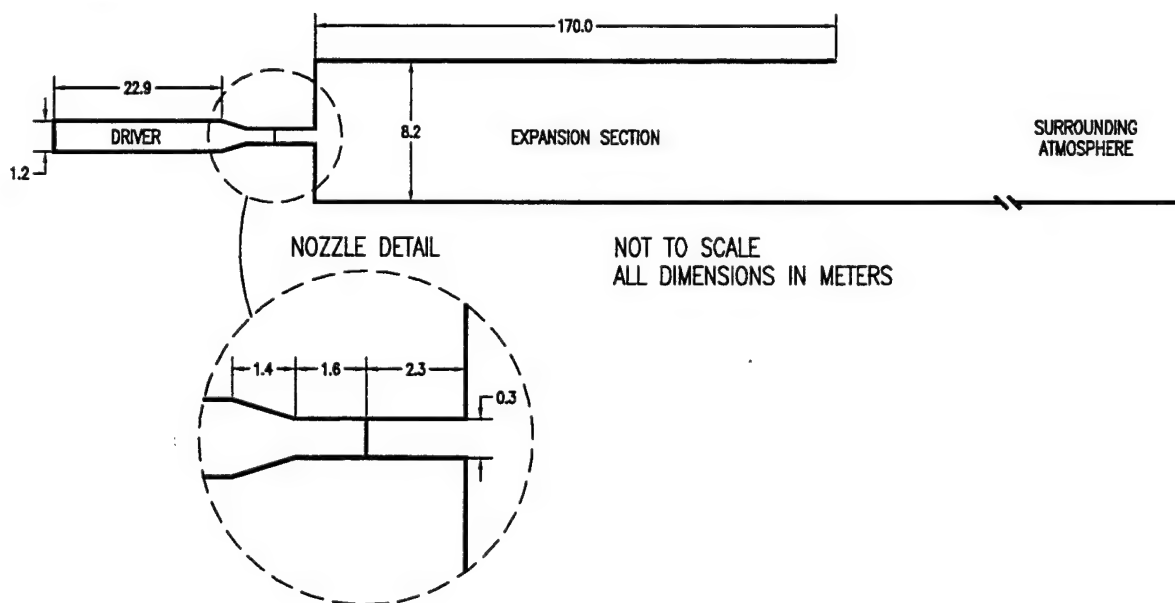

Figure 12. 2-D Planar Computational Model.

The only case simulated with the planar symmetry model was that with the driver overpressure of 15.5 MPa. The dynamic pressure history at a location 40 m down stream from the tunnel exit is compared to the result from the axisymmetric model in Figure 13. This figure shows that the two significant differences between the results of the planar and

11

axisymmetric models are the earlier arrival time and greater initial amplitude of the dynamic pressure from the planar symmetry calculation. Both of these differences are a result of the limited expansion of the shock in the planar case as compared to the spherical expansion in the axisymmetric case. The speed of a shock wave is proportional to the ratio of the pressures on either side of the shock.[10]After exiting the expansion tunnel, the leading shock in the planar symmetry calculation is not allowed to expand as much as that in the axisymmetric calculation, resulting in a greater average shock wave velocity in the planar symmetry case, and thus, an earlier arrival at the monitoring station.
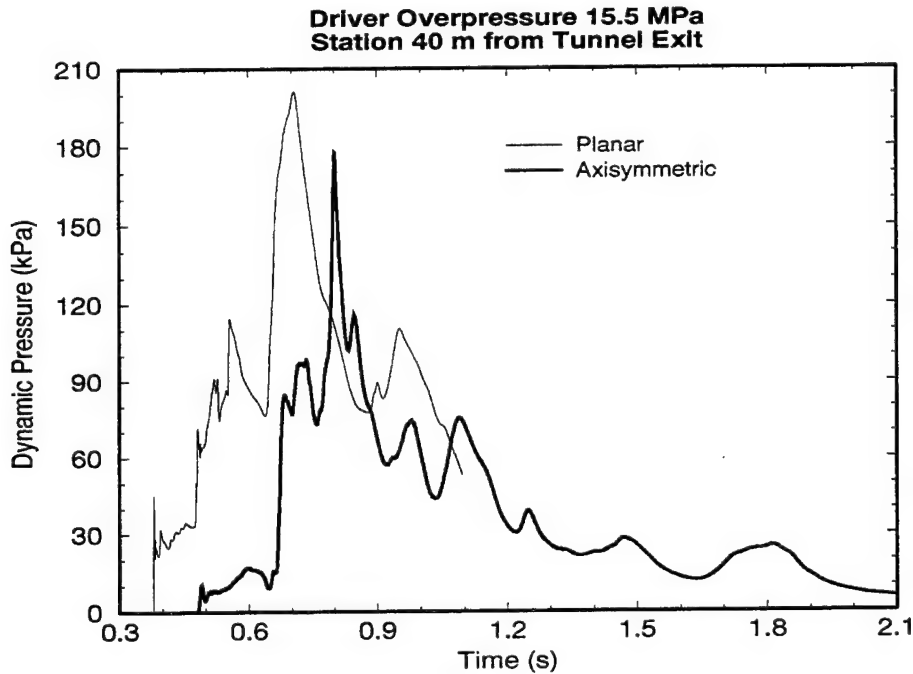
Figure 13. 2-D Planar and Axisymmetric Models: Dynamic Pressure Histories.

The velocity history from the planar symmetry calculation is plotted in Figure 14 and the Mach number history can be seen in Figure 15. These figures show a peak velocity of 600 m/s and a peak Mach number of 1.9 occurring at a time of 560 ms after flow initiation. The timing of this peak flow speed logically coincides with the peak dynamic pressure of the planar symmetry result shown in Figure 13.

To illustrate the expansion of the leading shock with increasing distance from the exit plane of the tunnel, the incident static overpressures are plotted as a function of distance in Figure 16. This figure shows that the amplitude of the incident shock realized by a target is a function of the placement of that target relative to the exit plane of the LB/TS. This suggests that in testing equipment in the exit jet, the target could be strategically positioned so that it would be exposed to a particular shock strength. However, care would have to be taken so that the target was not exposed to the negative velocities associated with the inflow phase that occurs in late time. The shaded region represented in Figure 16 is composed of the results of the axisymmetric and planar symmetry models for the case in

Driver Overpressure 15.5 MPa
2–D Planar – Station 40 m from Tunnel Exit
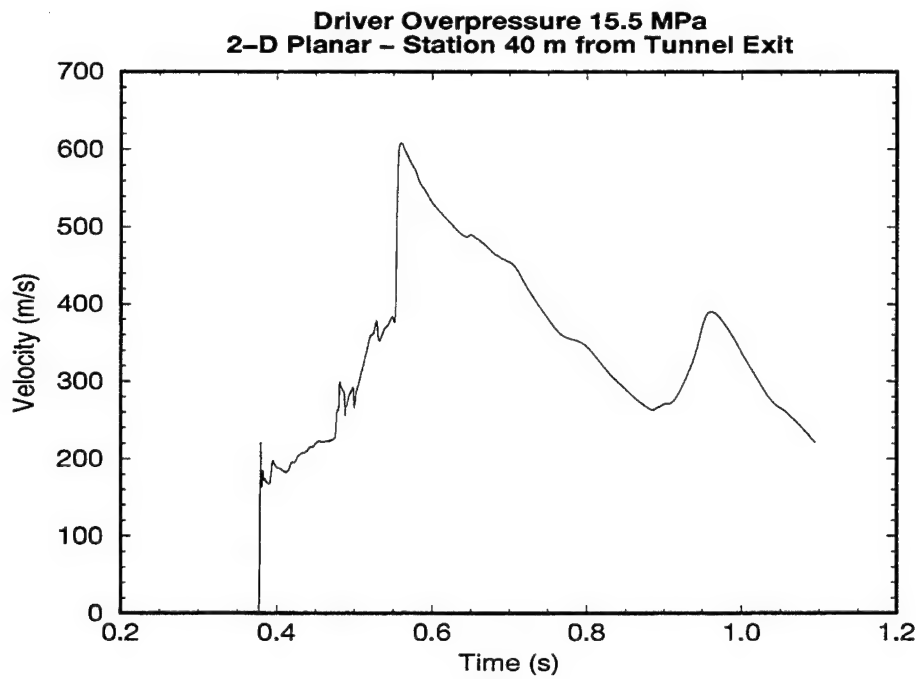
Figure 14. 2-D Planar Model: Velocity History.

Driver Overpressure 15.5 MPa
2–D Planar – Station 40 m from Tunnel Exit
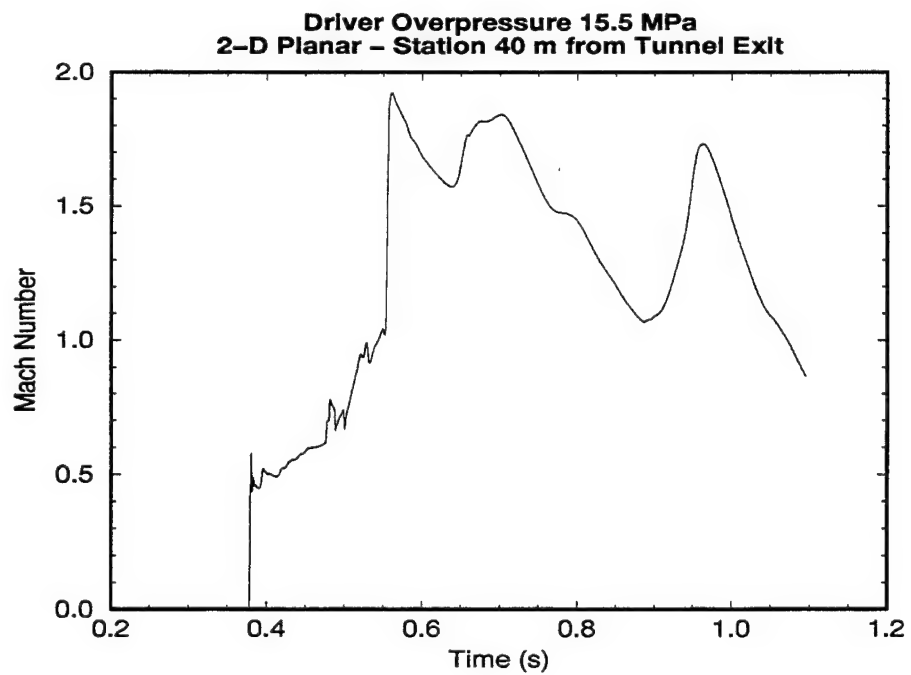
Figure 15. 2-D Planar Model: Mach Number History.

13

which the initial driver overpressure was 15.5 MPa. The upper limit on the shock amplitude is determined by the results of the planar symmetry calculation as this geometry allows the shock to expand only the longitudinal direction, away from the exit plane and vertically, away from the ground plane. The lower bound on the region is defined by the results of the axisymmetric calculation as this geometry allows the shock to expand spherically once exiting the expansion section. The two geometries produce the same level of shock amplitude inside the tunnel, explaining the convergence of the two curves at the tunnel exit. At large distances from the expansion tunnel exit, the shock has expanded to the point where its strength is insignificant to equipment testing as illustrated in the convergence of the upper and lower curves near the lower right corner of the graph.
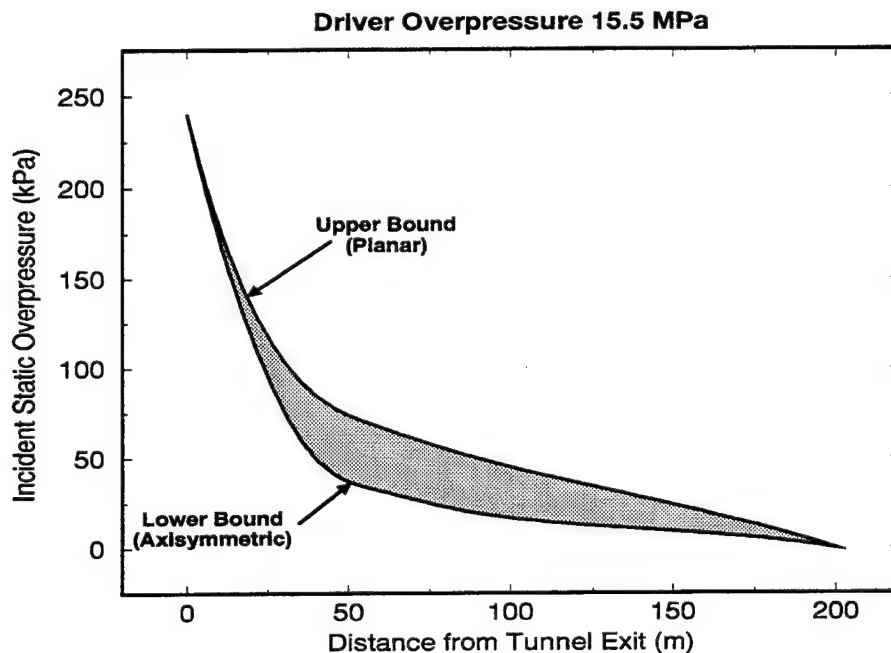
Figure 16. 2-D Planar and Axisymmetric Models: Incident Static Overpressure.

4.   3-D CALCULATIONS

With the 2-D calculations providing the initial estimates of the exit jet characteristics, the final step in the study was to construct a 3-D computational model to properly represent the LB/TS geometry. Representation of the shock tube in 3-D allows for the most accurate simulation of the expansion of the leading shock from the tunnel, into the surrounding atmosphere. Proper simulation of this expansion process will lead to the most accurate simulation of the formation and evolution of the exit jet.

The unified solution algorithms real gas[11] (USA-RG) code was the flow solver used for the 3-D calculations. USA-RG is an implicit, finite volume[7], Navier-Stokes[8] technique developed by the Rockwell Science Center. A 3-D, multiple block, generalized, curvilinear coordinate

14

system is used to discretize the computational domain for the USA-RG code. This type of discretization is sometimes referred to as a "body conformal" coordinate system since the distribution of grid points in space is used to describe the shape of the geometry being considered.

The 3-D, multiple block, curvilinear grid for the LB/TS is shown in Figures 17 and 18. The first of these two figures shows the upstream end of the computational domain, where the drivers interface with the expansion tunnel. The geometry of the LB/TS is symmetric about the vertical plane in the center of the expansion tunnel. This geometric symmetry allows the 3-D model to represent only half of the actual geometry with a symmetry boundary condition at the vertical center plane.

As stated earlier, the driver system of the LB/TS consists of nine sets of cylindrical tubes and converging nozzles. To reduce the number of grid points in the model and the required time to complete a simulation, the nine individual driver tubes were combined in the model into two banks of equivalent drivers. The bottom driver shown in Figure 17 is equivalent in volume and cross-sectional area to the five largest drivers of the LB/TS, while the top driver in the model represents the four smallest LB/TS driver tubes. While it is possible to model each driver tube individually, this level of model fidelity would require a much larger number of grid points than the combined two-driver model shown. This conservation of grid points significantly reduces the time required to complete a solution. This abstraction of the model is considered acceptable because the flow of interest to the current study is in the exit jet. Previous study of shock tubes with multiple drivers[12] has shown that the individual driver flows coalesce into a uniform flow field before reaching the test section. In the case of the LB/TS, the test section is located 105 m from the upstream end of the expansion tunnel and the length of the tunnel is 170 m. Thus, flow of gas in the tunnel is known to be uniform before its exit in forming the jet.

The downstream end of the expansion tunnel and the modeling of the surrounding atmosphere can be seen in Figure 18. This figure shows the relative scales of the driver system, expansion tunnel, and surrounding atmosphere as represented in the model. Also evident in the figure is the clustering of grid points in the area of the expansion tunnel and exit jet, with large grid spacing far away from the areas of interest. This view of the 3-D geometry also shows that the ground plane down stream from the tunnel exit is modeled as a flat surface with the same elevation as the expansion tunnel floor.

The first calculation performed with the 3-D model used an initial driver overpressure of 3.4 MPa and initial driver temperature of 288 K, matching the driver conditions of the first axisymmetric case. Figures 19 and 20 are presented to illustrate the evolution of the velocity field between times of 670 ms and 920 ms after flow initiation. The flow field at 670 ms shows the region of highest velocity located less than one tunnel diameter down stream from the exit plane of the expansion section. Then, at 920 ms, this region of high velocity has migrated to a position that is two to three tunnel diameters down stream from the tunnel exit.

To illustrate the uniformity of the flow in the region of interest, static overpressure and dynamic pressure histories are plotted in Figures 21 and 22 from two different stations at a
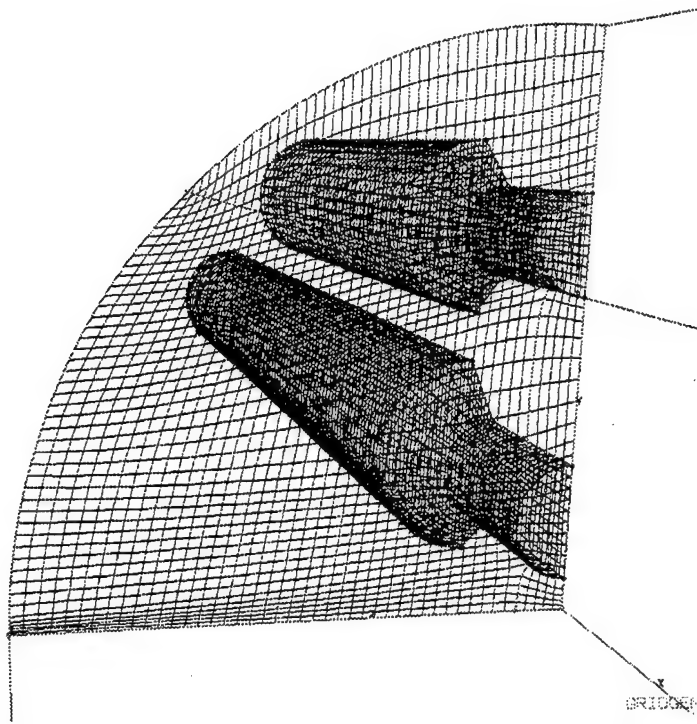
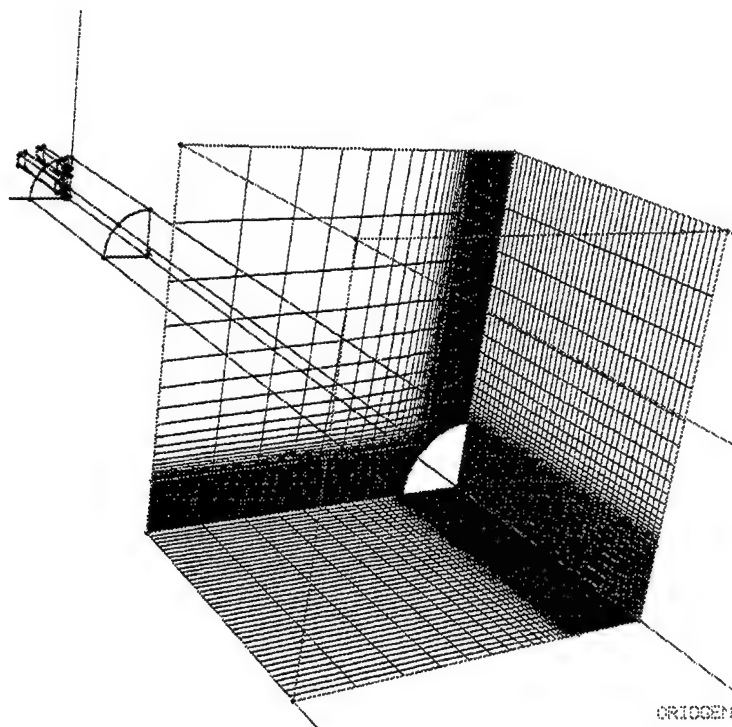Figure 17. 3-D Computational Model: Upstream End.
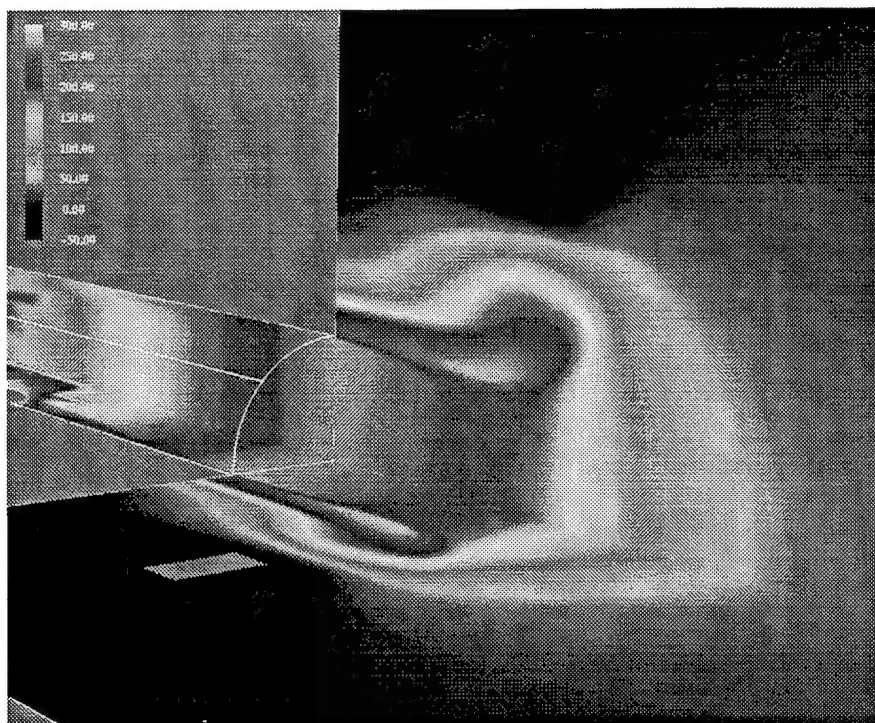

Figure 18. 3-D Computational Model.

16

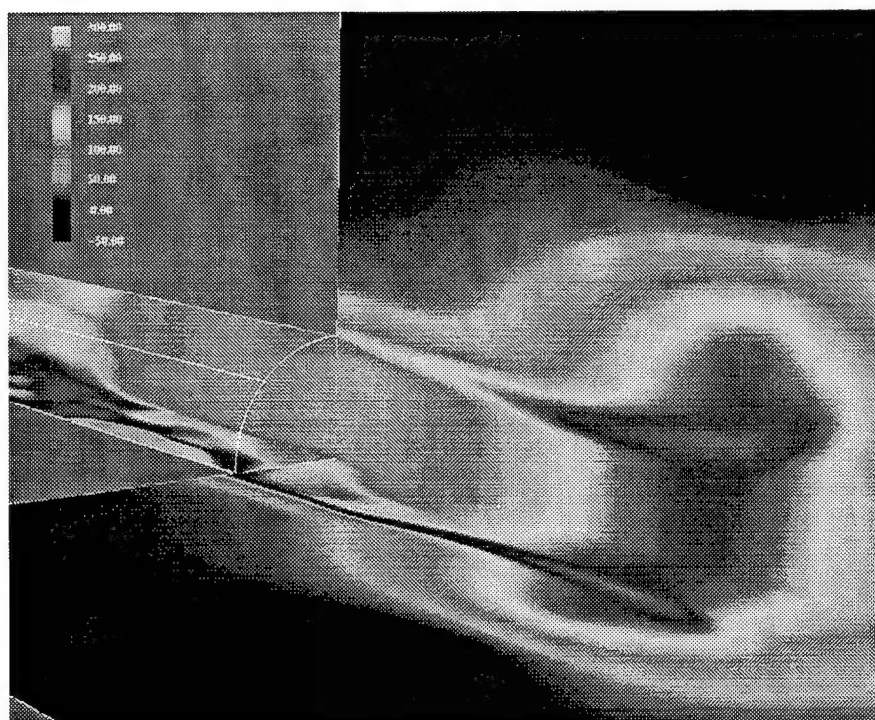Figure 19. 3-D Model: Velocity Profile at 670 ms.

Figure 20. 3-D Model: Velocity Profile at 920 ms.

position 40 m down stream from the tunnel exit. In the computational model, the X axis points in longitudinal direction with the origin at the upstream end of the expansion tunnel. The station locations specified in the figures are denoted by their Y and Z coordinates. The first station, with coordinates of (0,0) corresponds to a position in the center of the projected area of the tunnel at the ground surface. The other station is located 3 m above the ground plane and 3 m away from the center plane in the horizontal direction. This spread of station coordinates covers the most likely area to be used for target testing. The static overpressure and dynamic pressure histories from these two stations show that the exit jet flow is highly uniform in the region of interest to equipment testing.

Comparison of these 3-D results to the axisymmetric calculation results in Figure 8 confirms the earlier statement that the axisymmetric geometry produces the lower bound on shock amplitude in the exit jet. The incident shock in the axisymmetric case in Figure 8 is approximately 12 kPa, while that from the 3-D calculation is approximately 16 kPa. Comparison of the axisymmetric dynamic pressure history of Figure 9 with that of the 3-D calculation in Figure 22 shows that the axisymmetric calculation produces a greater peak dynamic pressure than the 3-D calculation but also decays more rapidly than that of the 3-D calculation. At a time of 1.2 s after flow initiation, the axisymmetric calculation has achieved a dynamic pressure impulse of 7.4 kPa-s, while the 3-D calculation has reached an impulse of 8.4 kPa-s at the same time. The slightly higher impulse of the 3-D calculation can be attributed to the presence of the flat ground plane.

Figure 23 is presented to again illustrate the dramatic change in the static overpressure histories with increasing distance from the exit plane of the expansion tunnel. For an initial driver overpressure of 3.4 MPa, the static overpressure history 20 m from the tunnel exit has an incident amplitude of 37 kPa and a positive phase duration of approximately 160 ms. At the 40-m position, the incident overpressure has decreased to 17 kPa but has a greater positive phase duration of 300 ms.

The next calculation performed with the 3-D model simulated an initial driver overpressure of 15.5 MPa and temperature of 288 K to match the 2-D axisymmetric and planar calculations at the maximum operational limit of the LB/TS. The static overpressure recorded at the station 40 m from the tunnel exit is presented in Figure 24. The incident static overpressure produced by this calculation was approximately 48 kPa. This almost exactly matches the value of the lower bound curve of Figure 16 at the same distance while the upper bound defined by the planar calculation is approximately 80 kPa.

The dynamic pressure, velocity, and Mach number histories for this calculation are presented in Figures 25, 26, and 27, respectively. In each of these figures, the peak value occurs at a time of approximately 600 ms. The peak dynamic pressure of 125 kPa is less than that of the 2-D calculations and, like the 3.4-MPa case, has a slower decay than its 2-D counterpart. The maximum velocity in the exit jet for the 15.5-MPa case was approximately 420 m/s, corresponding to a peak Mach number of 1.4. The dynamic pressure impulse at the end of the event has reached a level of approximately 77 kPa-s. This level of impulse is in the maximum range of that measured on above ground nuclear weapons tests of the 1950s and 1960s.[13]
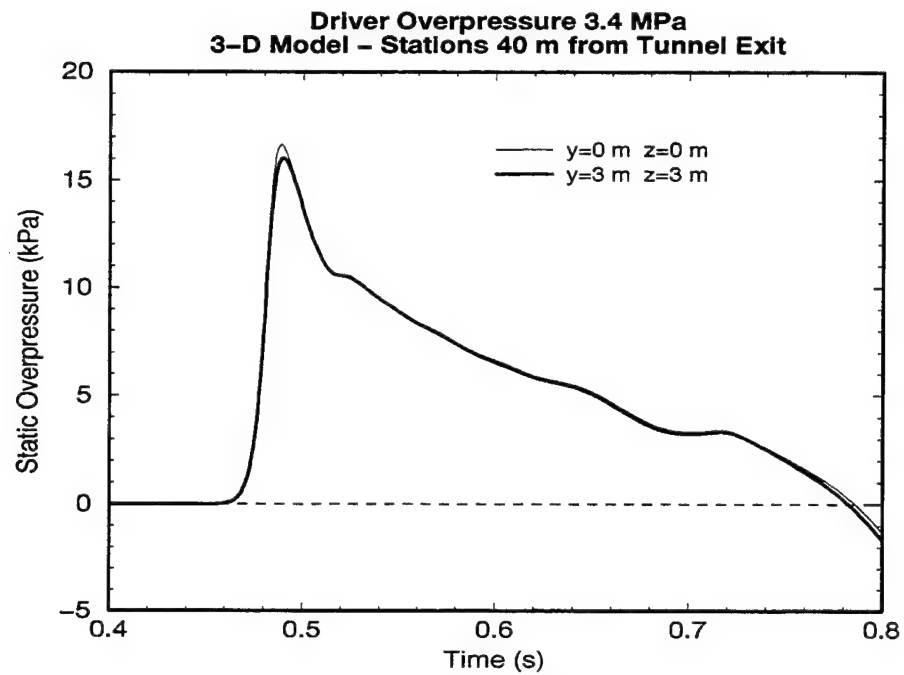
Figure 21. 3-D Model: Uniformity of Static Overpressure at 40 m.
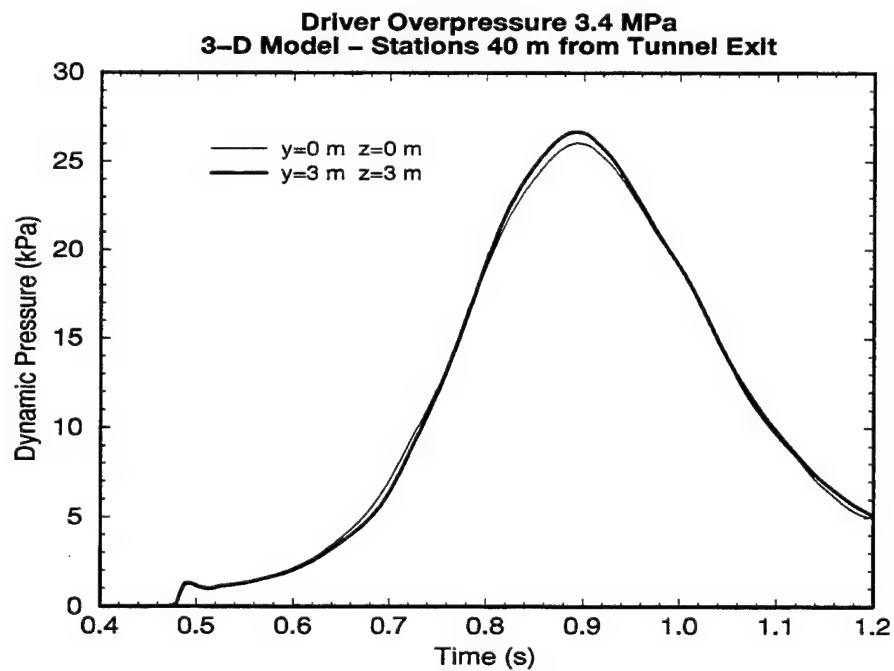
Figure 22. 3-D Model: Uniformity of Dynamic Pressure at 40 m.

19
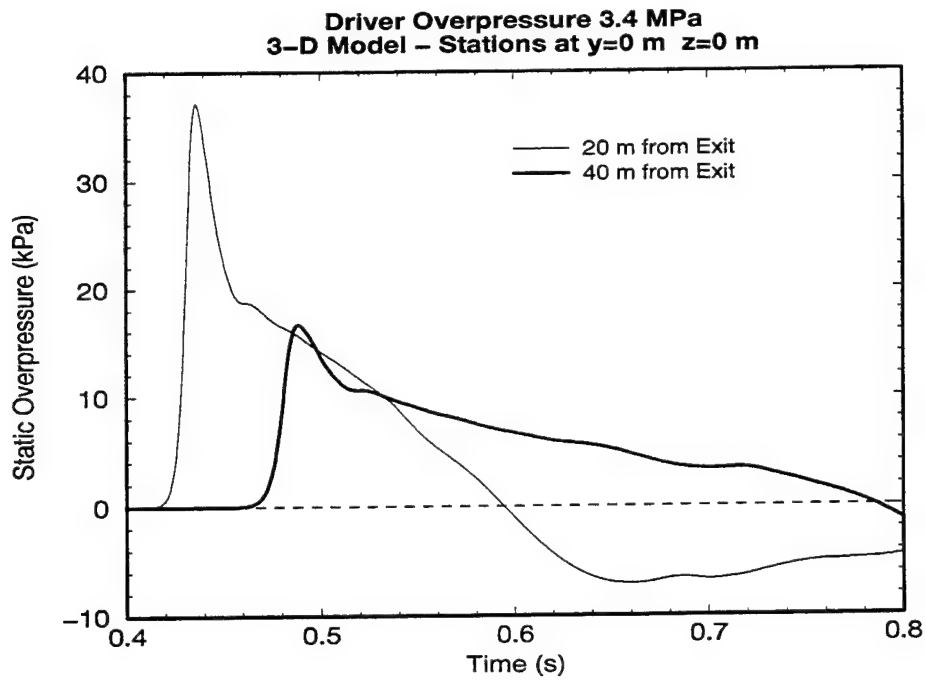
Figure 23. 3-D Model: Variation of Static Overpressure with Distance.
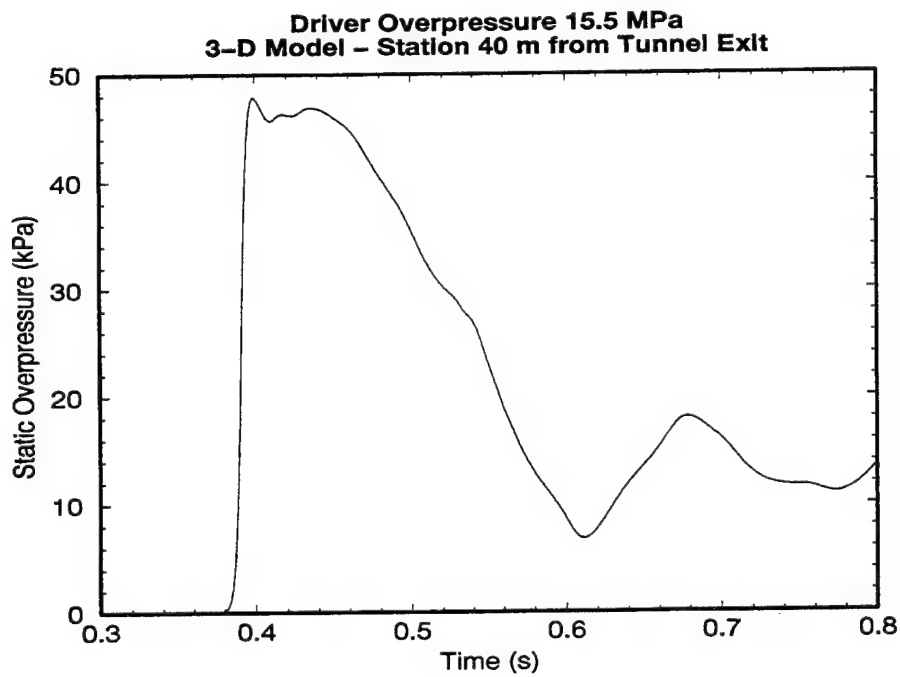
Figure 24. 3-D Model: Static Overpressure History.

20

Driver Overpressure 15.5 MPa
3-D Model – Station 40 m from Tunnel Exit
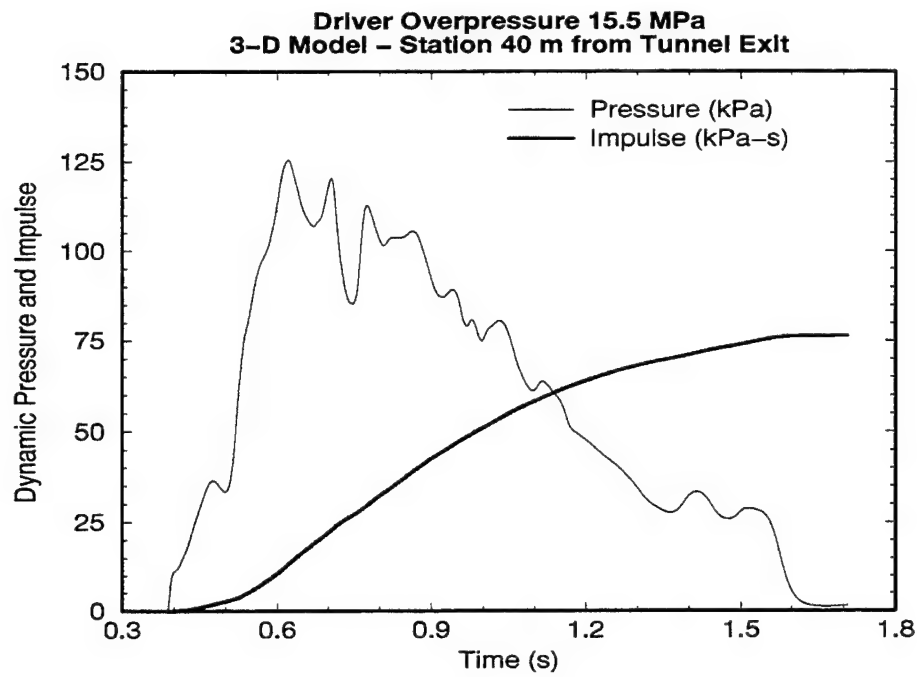
Figure 25. 3-D Model: Dynamic Pressure History.

Driver Overpressure 15.5 MPa
3-D Model – Station 40 m from Tunnel Exit
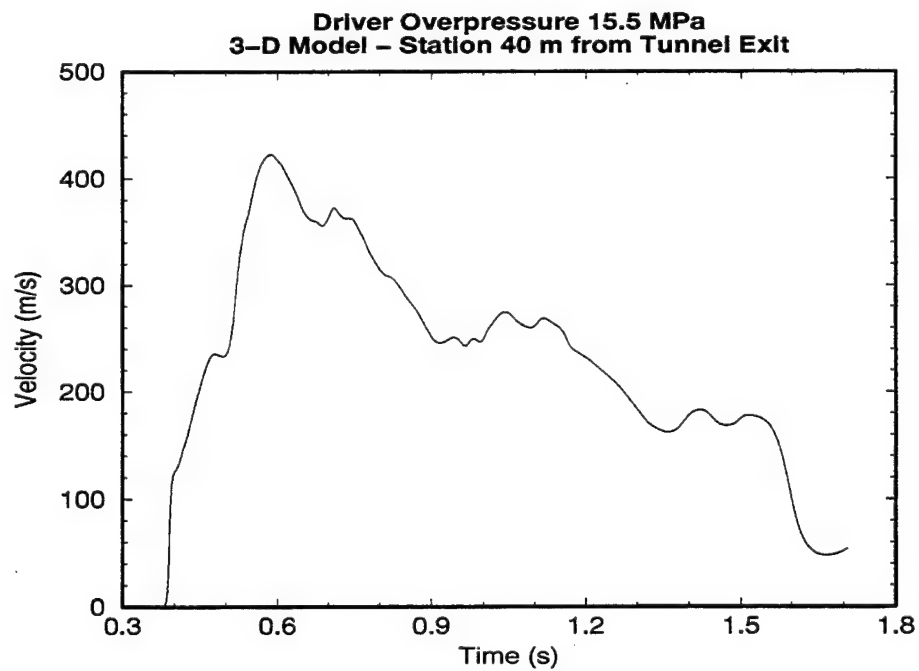
Figure 26. 3-D Model: Velocity History.

21

Driver Overpressure 15.5 MPa
3–D Model – Station 40 m from Tunnel Exit
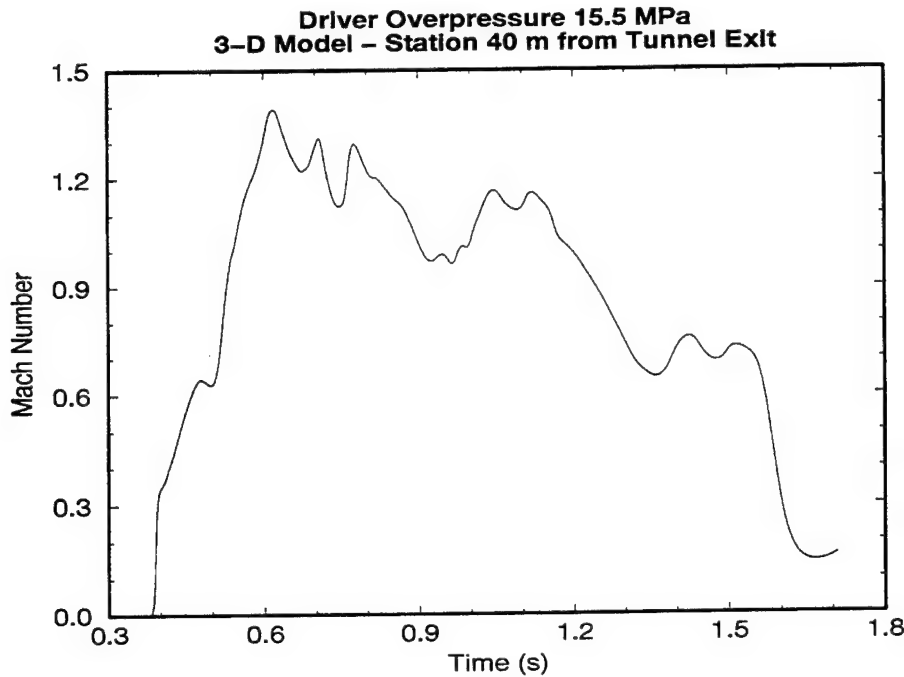
Figure 27. 3-D Model: Mach Number History.

The final calculation in the study was performed in an attempt to match the dynamic pressure history in the LB/TS exit jet to the measured data from a nuclear test. This calculation employed an initial driver overpressure of 6.2 MPa and an initial driver gas temperature of 288 K. The resulting blast wave history data were compared to those of the nuclear test MET[14] of 1955 in which a 22.0-kT device was detonated 122 m above the desert surface of the Nevada Test Site. Figure 28 provides the comparison between the dynamic pressure histories of the exit jet and the nuclear test. The exit jet history was recorded at a location 10 m from the exit plane of the LB/TS expansion tunnel. The MET data were measured at a distance of 762 m from ground zero. In the original nuclear data, a time of zero corresponded to the arrival of the leading shock at the gauge. In Figure 28, the time base of the nuclear data has been shifted to correspond to the arrival time of the leading shock at the 10-m station down stream from the exit plane of the expansion tunnel. The figure shows the peak dyamic pressure of the nuclear data to be 66.2 kPa, while that of the exit jet flow is 64.9 kPa. The exit jet history also exhibits rates of dynamic pressure increase and decrease on either side of the peak that are similar to those changes in the test data. Thus, the ability of the exit jet to simulate the dynamic pressure history of the nuclear test is an indication that it will produce the whole body response of military equipment that would be anticipated on a nuclear battlefield.

Driver Overpressure 6.2 MPa
3–D Model – Station 10 m from Tunnel Exit
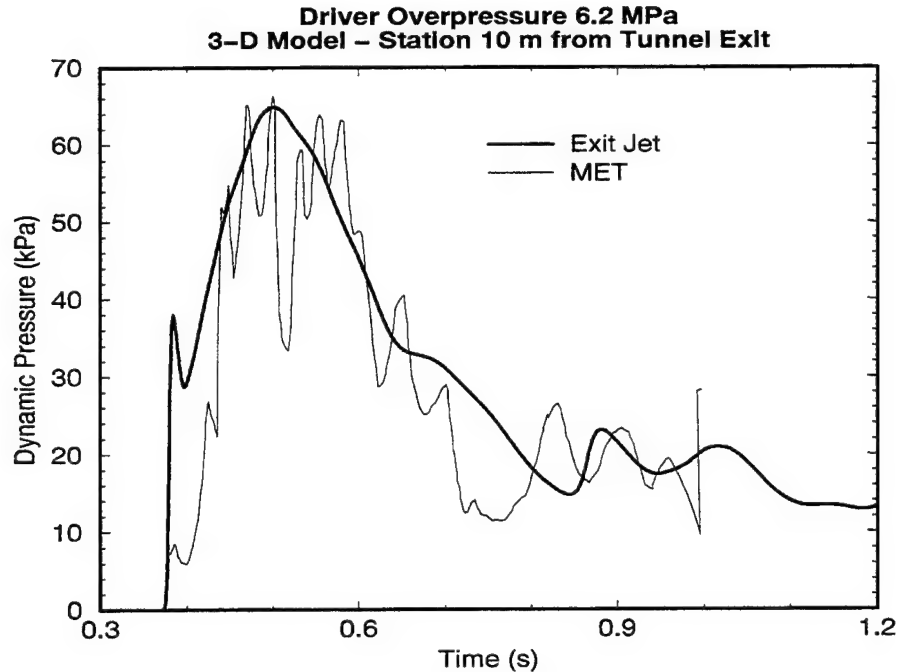
Figure 28. 3-D Model: Dynamic Pressure History Compared to Nuclear Test Data.

5. SUMMARY

The computational study presented in this report was performed to determine the major characteristics of the jet flow exiting the expansion tunnel of the LB/TS. The 2-D planar and axisymmetric calculations provided upper and lower limits on the amplitude of the incident static overpressure at different distances from the exit plane of the expansion tunnel. These calculations also served to provide initial predictions of the shapes of the pressure histories and the possible energy delivery in the jet as a function of initial driver overpressure.

The 3-D calculations used the findings of the preliminary 2-D calculations to further refine the definitions of the exit jet wave shapes and determine the uniformity of the flow field in the positions of interest to equipment testing.

In all the 2-D planar and 3-D computations in the study, the ground surface down stream from the tunnel exit was represented as a perfectly flat plane at the same elevation as the expansion tunnel floor. In the actual LB/TS geometry, the ground plane is not flat and is lower than the floor of the expansion tunnel. If it is decided that the LB/TS exit jet technique will be used for equipment testing, additional study will be required to determine the ground plane configuration that would produce a useful, coherent exit jet at minimum cost.

The dynamic pressure impulse delivered in the exit jet at the maximum operational limits of the LB/TS is similar to levels measured on nuclear weapons test where the non-ideal blast effect was known to exist. The dynamic pressure history of the exit jet was also

23

shown to closely resemble the measured data from a nuclear test from 1955. Additionally, the computational study revealed a strong relationship between shock amplitude in the exit jet and distance from the exit plane of the expansion tunnel. Combining these known characteristics of the exit jet allows one to obtain desired test parameters through careful selection of initial driver overpressure and target placement relative to the exit plane of the tunnel to balance the delivery of static overpressure and dynamic pressure histories desired for the target.

REFERENCES

1. Glasstone, S. and P. Dolan - Editors. "The Effects of Nuclear Weapons." Department of Army Pamphlet No. 50-3, HQ, Department of Army. March 1977.

2. Kennedy, L. et al. - Editors "Capabilities of Nuclear Weapons, Chapter 2-Airblast Phenomena, Section 2II-Airblast Over Real Surfaces." DNA001-87-C-0141, Defense Nuclear Agency, Washington, DC. August 1988.

3. Schraml, S.J. "Performance Predictions for the Large Blast/Thermal Simulator Based on Experimental and Computational Results." U.S. Army Ballistic Research Laboratory Technical Report BRL-TR-3232. Aberdeen Proving Ground, MD. May 1991.

4. Schraml, S.J. and R.J. Pearson. "Small Scale Shock Tube Experiments Using a Computer Controlled Active Rarefaction Wave Eliminator." U.S. Army Ballistic Research Laboratory Technical Report BRL-TR-3149. September 1990.

5. Loucks, R.B. et al. "Simulation of Non-Ideal Blast with a Shock Tube Exit Jet." U.S. Army Research Laboratory Technical Report ARL-TR-984. Aberdeen Proving Ground, MD. February 1996.

6. Hikida, S., R. Bell, and C. Needham. "The SHARC Codes: Documentation and Sample Problems." S-Cubed Technical Report SSS-R-89-9878. September 1988.

7. Fletcher, C.A.J. *Computational Techniques for Fluid Dynamics - Volume I.* Springer-Verlag. ISBN 3-540-53601-9 1991.

8. Kundu, P.K. "Fluid Mechanics." Academic Press, Inc. San Diego, CA. 1990.

9. Barthel, J. "2-D Hydrocode Computations Using a k-ϵ Turbulence Model: Model Description and Test Calculations." S-Cubed Technical Report SSS-TR-85-7115. June 1985, (Footnotes added August 1988).

10. Zucrow, M.J. and J.D. Hoffman. *Gas Dynamics.* John Wiley & Sons. New York, NY. ISBN 0-471-98440-X. 1976.

11. Chakravarthy, S., K. Szema, U. Goldberg, J. Gorski and S. Osher. "Application of a New Class of High Accuracy TVD Schemes to the Navier-Stokes Equations." AIAA Paper 85-0165. January 1985.

12. Schraml, S.J. and C. Mermagen. "Experimental Evaluation and Numerical Simulations of Multi-Driver Shock Tube Flow." U.S. Army Research Laboratory Technical Report ARL-TR-1084. Aberdeen Proving Ground, MD. April 1996.

13. Ethridge, N.H. et al. "Real Surface (Non-Ideal) Effects on Nuclear Explosion Airblast from PRISCILLA-Type Events." U.S. Army Research Laboratory Contract Report ARL-CR-277. October 1995.

14. Shelton, F.H. *Reflections of a Nuclear Weaponeer.* Shelton Enterprises. Colorado Springs, CO. 1988.

INTENTIONALLY LEFT BLANK

NO. OF COPIES	ORGANIZATION
2	ADMINISTRATOR DEFENSE TECHNICAL INFO CENTER ATTN DTIC DDA 8725 JOHN J KINGMAN RD STE 0944 FT BELVOIR VA 22060-6218
1	DIRECTOR US ARMY RESEARCH LABORATORY ATTN AMSRL OP SD TA/ RECORDS MANAGEMENT 2800 POWDER MILL RD ADELPHI MD 20783-1197
1	DIRECTOR US ARMY RESEARCH LABORATORY ATTN AMSRL OP SD TL/ TECHNICAL LIBRARY 2800 POWDER MILL RD ADELPHI MD 207830-1197
1	DIRECTOR US ARMY RESEARCH LABORATORY ATTN AMSRL OP SD TP/ TECH PUBLISHING BRANCH 2800 POWDER MILL RD ADELPHI MD 20783-1197
2	HQDA (SARD TR/MS K KOMINOS) (SARD TR/DR R CHAIT) WASHINGTON DC 20310-0103
2	DIRECTOR FEDERAL EMERGENCY MGMT AGENCY ATTN PUBLIC RELATIONS OFFICE TECHNICAL LIBRARY WASHINGTON DC 20472
2	HQDA (SARD TT/MS C NASH) (SARD TT/DR F MILTON) WASHINGTON DC 20310-0103
1	CHAIRMAN DOD EXPLOSIVES SAFETY BOARD ROOM 856 C HOFFMAN BLDG 1 2461 EISENHOWER AVENUE ALEXANDRIA VA 22331-0600
1	DIRECTOR OF DEFENSE RESEARCH AND ENGINEERING ATTN DD/TWP WASHINGTON DC 20301

NO. OF COPIES	ORGANIZATION
1	DIRECTOR DEFENSE INTELLIGENCY AGENCY ATTN DT 2/WPNS & SYS DIVISION WASHINGTON DC 20301
1	ASST SECRETARY OF DEFENSE (ATOMIC ENERGY ATTN DOCUMENT CONTROL WASHINGTON DC 20301

6	DIRECTOR
	DEFENSE NUCLEAR AGENCY
	ATTN CSTI TECHNICAL LIBRARY
	  ESA W SUMMA
	      E SEIDEN
	      K PETERSEN
	  WEP T KENNEDY
	      M FRANKEL
	WASHINGTON DC 20305

1	CHAIRMAN JOINT CHIEFS OF STAFF ATTN J 5 R&D DIVISION WASHINGTON DC 20301
2	DA DCSOPS ATTN TECHNICAL LIBRARY DIR OF CHEM & NUC OPS WASHINGTON DC 20310

4	COMMANDER
	FIELD COMMAND DNA
	ATTN FCTTS E MARTINEZ
	      FCTOSL F MOYNIHAN
	      FCTIH H ROSS
	      FCTIH W BRENNAN
	KIRTLAND AFB NM 87115

10	CENTRAL INTELLIGENCE AGENCY DIR/DB/STANDARD ATTN GE 47 HQ WASHINGTON DC 20505
1	DIRECTOR ADVANCED RSCH PROJECTS AGENCY ATTN TECHNICAL LIBRARY 3701 NORTH FAIRFAX DRIVE ARLINGTON VA 22203-1714
2	COMMANDER US ARMY CECOM ATTN AMSEL RD AMSEL RO TPPO P FORT MONMOUTH NJ 07703-5301

NO. OF COPIES	ORGANIZATION
1	COMMANDER US ARMY CECOM R&D TECHNICAL LIBRARY ATTN ASQNC ELC IS L R MYER CTR FORT MONMOUTH NJ 07703-5000
1	MIT ATTN TECHNICAL LIBRARY CAMBRIDGE MA 02139
1	COMMANDER US ARMY FSTC ATTN RESEARCH & DATA BRANCH 220 7TH STREET NE CHARLOTTESVILLE VA 22901-5396
1	COMMANDER US ARMY ARDEC ATTN SMCAR FSM W/BARBER BLDG94 PICATINNY ARSENAL NJ 07806-5000
1	DIRECTOR US ARMY MISSILE & SPACE INTELLIGENCE CENTER ATTN AIAMS YDL REDSTONE ARSENAL AL 35898-5500
1	COMMANDING OFFICER (CODE L51) NAVAL CIVIL ENGINEERING LAB ATTN J TANCRETO PORT HUENEME CA 93043-5003
2	COMMANDER US ARMY STRATEGIC DEFENSE CMD ATTN CSSD H MPL TECH LIB CSSD H XM DR DAVIES PO BOX 1500 HUNTSVILLE AL 35807
2	COMMANDER US ARMY CORPS OF ENGINEERS WATERWAYS EXPERIMENT STA ATTN CEWES SS R J WATT CEWES TL TECH LIBRARY PO BOX 631 VICKSBURG MS 39180-0631
1	COMMANDER US ARMY ENGINEER DIVISION ATTN HNDED FD PO BOX 1500 HUNTSVILLE AL 35807

NO. OF COPIES	ORGANIZATION
3	COMMANDER US ARMY NUCLEAR & CHEM AGENCY 7150 HELLER LOOP SUITE 101 SPRINGFIELD VA 22150-3198
1	COMMANDER US ARMY CORPS OF ENGINEERS FT WORTH DISTRICT ATTN CESWF PM J PO BOX 17300 FORT WORTH TEXAS 76102-0300
1	DIRECTOR TRAC FLVN ATTN ATRC FORT LEAVENWORTH KS 66027-5200
1	COMMANDER US ARMY RESEARCH OFFICE ATTN SLCRO D PO BOX 12211 RESEARCH TRIANGLE PARK NC 27709-2211
1	DIRECTOR HQ TRAC RPD ATTN ATRC RPR RADDA FORT MONROE VA 23651-5143
2	OFFICE OF NAVAL RESEARCH ATTN DR A FAULSTICK CODE 23 800 N QUINCY STREET ARLINGTON VA 22217
1	DIRECTOR TRAC WSMR ATTN ATRC WC KIRBY WSMR NM 88002-5502
2	COMMANDER US ARMY WSMR ATTN STEWS NED (DR MEASON) STEWS DATTS O (RL PENNY) WSMR NM 88002-5158
2	CHIEF OF NAVAL OPERATIONS DEPARTMENT OF THE NAVY ATTN OP 03EG OP 985F WASHINGTON DC 20350
1	COMMANDER DAVID TAYLOR RESEARCH CENTER ATTN CODE 522 TECH INFO CTR BETHESDA MD 20084-5000

NO. OF COPIES	ORGANIZATION	NO. OF COPIES	ORGANIZATION
1	OFFICER IN CHARGE (CODE L31) CIVIL ENGINEERING LABORATORY NAVAL CONST BATTALION CENTER ATTN TECHNICAL LIBRARY PORT HUENEME CA 93041	2	AIR FORCE ARMAMENT LAB ATTN AFATL/DOIL AFATL/DLYV EGLIN AFB FL 32542-5000
1	COMMANDER (CODE 533) NAVAL WEAPONS CENTER ATTN TECHNICAL LIBRARY CHINA LAKE CA 93555-6001	1	DIRECTOR IDAHO NATIONAL ENGINEERING LAB ATTN SPEC PROGRAMS J PATTON 2151 NORTH BLVD MS 2802 IDAHO FALLS ID 83415
1	COMMANDER DAHLGREN DIVISION NAVAL SURFACE WARFARE CENTER ATTN CODE E23 LIBRARY DAHLGREN VA 22448-5000	3	PHILLIPS LABORATORY (AFWL) ATTN NTE NTED NTES KIRTLAND AFB NM 87117-6008
1	COMMANDER NAVAL RESEARCH LABORATORY ATTN CODE 2027 TECH LIBRARY WASHINGTON DC 20375	1	DIRECTOR LAWRENCE LIVERMORE NATL LAB ATTN TECH INFO DEPT L 3 PO BOX 808 LIVERMORE CA 94550
1	OFFICER IN CHARGE WHITE OAK WARFARE CENTER DETACHMENT ATTN CODE E232 TECH LIBRARY 10901 NEW HAMPSHIRE AVENUE SILVER SPRING MD 20903-5000	1	NAIC/DXLA ATTN TECHNICAL LIBRARY 4180 WATSON WAY WRIGHT PATTERSON AFB OH 45433-5648
1	AL/LSCF ATTN J LEVINE EDWARDS AFB CA 93523-5000	1	DIRECTOR NATL AERONAUTICS & SPACE ADMIN ATTN SCIENTIFIC & TECH INFO FAC PO BOX 8757 BWI AIRPORT BALTIMORE MD 21240
1	COMMANDER NAVAL WEAPONS EVALUATION FAC ATTN DOCUMENT CONTROL KIRTLAND AFB NM 87117	3	KAMAN SCIENCES CORPORATION ATTN LIBRARY PA ELLIS FH SHELTON PO BOX 7463 COLORADO SPRINGS CO 80933-7463
1	RADC (EMTLD/DOCUMENT LIB) GRIFFISS AFB NY 13441		
1	AEDC ATTN R MCAMIS MAIL STOP 980 ARNOLD AFB TN 37389	4	DIRECTOR IDAHO NATIONAL ENGINEERING LAB EG&G IDAHO INC ATTN R GUENZLER MS 3505 R HOLMAN MS 3510 R A BERRY W C REED PO BOX 1625 IDAHO FALLS ID 83415
1	OLAC PL/TSTL ATTN D SHIPLETT EDWARDS AFB CA 93523 5000		
1	AFIT/ENY ATTN LTC HASEN PHD WRIGHT PATTERSON AFB OH 45433-6583		

NO. OF COPIES	ORGANIZATION	NO. OF COPIES	ORGANIZATION

4	DIRECTOR
	SANDIA NATIONAL LABORATORIES
	ATTN DOC CONTROL 3141
	    D GARDNER DIV 1421
	    J MCGLAUN DIV 1541
	PO BOX 5800
	ALBUQUERQUE NM 87185-5800
		1	CARPENTER RESEARCH CORP
			ATTN H JERRY CARPENTER
			27520 HAWTHORNE BLVD SUITE 263
			PO BOX 2490
			ROLLING HILLS ESTATES CA 90274

2	LOS ALAMOS NATL LABORATORY MAIL STATION 5000 REPORT COLLECTION CID 14 MS P364 PO BOX 1663 LOS ALAMOS NM 87545	1	AEROSPACE CORPORATION ATTN TECH INFO SERVICES PO BOX 92957 LOS ANGELES CA 90009
1	REPORT COLLECTION CIC 14 MS P364 LOS ALAMOS NATL LABORATORY LOS ALAMOS NM 87545	1	THE BOEING COMPANY ATTN AEROSPACE LIBRARY PO BOX 3707 SEATTLE WA 98124
1	REPORT COLLECTION RESEARCH LIBRARY MS P362 PO BOX 7113 LOS ALAMOS NM 87544-7113	2	FMC CORPORATION ADVANCED SYSTEMS CENTER ATTN J DROTLEFF C KREBS MDP 95 BOX 58123 2890 DE LA CRUZ BLVD SANTA CLARA CA 95052
1	DIRECTOR SANDIA NATIONAL LABORATORIES LIVERMORE LABORATORY ATTN DOC CONTROL FOR TECH LIB PO BOX 969 LIVERMORE CA 94550	1	SVERDRUP TECHNOLOGY INC SVERDRUP CORPORATION AEDC ATTN BD HEIKKINEN MS 900 ARNOLD AFB TN 37389-9998
1	DIRECTOR NASA LANGLEY RESEARCH CENTER ATTN TECHNICAL LIBRARY HAMPTON VA 23665	1	DYNAMICS TECHNOLOGY INC ATTN D T HOVE G P MASON 21311 HAWTHORNE BLVD SUITE 300 TORRANCE CA 90503
2	APPLIED RESEARCH ASSOCIATES INC ATTN J KEEFER NH ETHRIDGE PO BOX 548 ABERDEEN MD 21001	1	KTECH CORPORATION ATTN DR E GAFFNEY 901 PENNSYLVANIA AVE NE ALBUQUERQUE NM 87111

4	APPLIED RESEARCH ASSOCIATES INC
	ATTN C NEEDHAM
	    J CREPEAU
	    S HIKIDA
	    R NEWELL
	4300 SAN MATEO BLVD
	ALBUQUERQUE NM 87110
		1	EATON CORPORATION
			DEFENSE VALVE & ACTUATOR DIV
			ATTN J WADA
			2338 ALASKA AVE
			EL SEGUNDO CA 90245-4896

1	ADA TECHNOLOGIES INC
	ATTN JAMES R BUTZ
	HONEYWELL CENTER SUITE 110
	304 INVERNESS WAY SOUTH
	ENGLEWOOD CO 80112
		2	MCDONNELL DOUGLAS ASTRO-
			    NAUTICS CORP
			ATTN R W HALPRIN
			    K A HEINLY
			5301 BOLSA AVENUE
			HUNTINGTON BEACH CA 92647

NO. OF COPIES	ORGANIZATION	NO. OF COPIES	ORGANIZATION
4	KAMAN AVIDYNE ATTN R RUETENIK S CRISCIONE R MILLIGAN T STAGLIANO 83 SECOND AVENUE NORTHWEST INDUSTRIAL PARK BURLINGTON MA 01830	1	METACOMP TECHNOLOGIES INC ATTN S CHAKRAVARTHY 650 WESTLAKE BLVD SUITE 203 WESTLAKE VILLAGE CA 91362
1	MDA ENGINEERING INC ATTN DR DALE ANDERSON 500 EAST BORDER STREET SUITE 401 ARLINGTON TX 07601	1	ORLANDO TECHNOLOGY INC ATTN D MATUSKA 60 SECOND STREET BLDG 5 SHALIMAR FL 32579
2	POINTWISE INC ATTN J CHAWNER J STEINBRENNER PO BOX 210698 BEDFORD TX 76095-7698	4	S CUBED A DIVISION OF MAXWELL LABS INC ATTN TECHNICAL LIBRARY R DUFF K PYATT J BARTHEL PO BOX 1620 LA JOLLA CA 92037-1620
2	PHYSICS INTERNATIONAL CORP PO BOX 5010 SAN LEANDRO CA 94577-0599	1	SAICORPORATION ATTN J GUEST 2301 YALE BLVD SE SUITE E ALBUQUERQUE NM 87106
2	KAMAN SCIENCES CORPORATION ATTN DASIAC (2CYS) PO DRAWER 1479 816 STATE STREET SANTA BARBARA CA 93102-1479	1	SUNBURST RECOVERY INC ATTN DR C YOUNG PO BOX 2129 STEAMBOAT SPRINGS CO 80477
1	LOGICON RDA ATTN GP GANONG PO BOX 9377 ALBUQUERQUE NM 87119	1	SVERDRUP TECHNOLOGY INC ATTN RF STARR PO BOX 884 TULLAHOMA TN 37388
1	LOGICON RDA ATTN B LEE 6053 W CENTURY BLVD LOS ANGELES CA 90045	1	S CUBED A DIVISION OF MAXWELL LABS INC ATTN JAMES SEVIER 2501 YALE BLVD SE ALBUQUERQUE NM 87106
1	LOCKHEED MISSILES & SPACE CO ATTN J J MURPHY DEPT 81 11 BLDG 154 PO BOX 504 SUNNYVALE CA 94086	3	SRI INTERNATIONAL ATTN DR GR ABRAHAMSON DR J GRAN DR B HOLMES 333 RAVENWOOD AVENUE MENLO PARK CA 94025
1	SCIENCE CENTER ROCKWELL INTERNATIONAL CORP ATTN S RAMAKRISHNAN D OTA 1049 CAMINO DOS RIOS PO BOX 2085 THOUSAND OAKS CA 91358	1	TRW BALLISTIC MISSILE DIVISION ATTN H KORMAN MAIL STATION 526/614 PO BOX 1310 SAN BERNADINO CA 92402

NO. OF COPIES	ORGANIZATION
1	BATTELLE ATTN TACTEC LIB JN KHIGGINS 505 KING AVENUE COLUMBUS OH 43201-2693
1	THERMAL SCIENCE INC ATTN R FELDMAN 2200 CASSENS DRIVE ST LOUIS MO 63026
2	DENVER RESEARCH INSTITUTE ATTN J WISOTSKI TECHNICAL LIBRARY PO BOX 10758 DENVER CO 80210
1	STATE UNIVERSITY OF NEW YORK MECH & AEROSPACE ENGINEERING ATTN DR PEYMAN GIVI BUFFALO NY 14260
2	UNIVERSITY OF MARYLAND INST FOR ADV COMPUTER STUDIES ATTN L DAVIS G SOBIESKI COLLEGE PARK MD 20742
1	CALIFORNIA INST OF TECHNOLOGY ATTN T J AHRENS 1201 E CALIFORNIA BLVD PASADENA CA 91109
1	UNIVERSITY OF MINNESOTA ARMY HIGH PERF COMP RES CTR ATTN DR TAYFUN E TEZDUYAR 1100 WASHINGTON AVE SOUTH MINNEAPOLIS MN 55415
3	SOUTHWEST RESEARCH INSTITUTE ATTN DR C ANDERSON S MULLIN A B WENZEL PO DRAWER 28255 SAN ANTONIO TX 78228-0255
2	COMMANDER US ARMY NRDEC ATTN SSCNC YSD (J ROACH) SSCNC WST (A MURPHY) KANSAS STREET NATICK MA 10760-5018

NO. OF COPIES	ORGANIZATION
	ABERDEEN PROVING GROUND
2	DIR ARL ATTN AMSRL OP AP L (TECH LIB) BLDG 305 APG
1	COMMANDER US ARMY TECOM ATTN AMSTE TE F (L TELETSKI) RYAN BLDG APG
1	COMMANDER US ARMY THAMA ATTN AMSTH TE APG -EA
1	COMMANDER US ARMY TEST CENTER ATTN STEC LI APG
15	DIRECTOR US ARMY RESEARCH LABORATORY ATTN AMSRL CI H C NIETUBICZ AMSRL CI HC J COLLINS J GROSH D HISLEY AMSRL IS B A MARK R PEARSON AMSRL SL CM E FIORVANTE AMSRL WM PB P PLOSTINS P WEINACHT B GUIDOS AMSRL WM TB R FREY R LOTTERO J STARKENBERG AMSRL WM TC W DEROSSET K KIMSEY

REPORT DOCUMENTATION PAGE

Public reporting burden for this collection of information is estimated to average 1 hour per response, including the time for reviewing instructions, searching existing data sources, gathering and maintaining the data needed, and completing and reviewing the collection of information. Send comments regarding this burden estimate or any other aspect of this collection of information, including suggestions for reducing this burden, to Washington Headquarters Services, Directorate for Information Operations and Reports, 1215 Jefferson Davis Highway, Suite 1204, Arlington, VA 22202-4302, and to the Office of Management and Budget, Paperwork Reduction Project (0704-0188), Washington, DC 20503.

1. AGENCY USE ONLY (Leave blank)	2. REPORT DATE	3. REPORT TYPE AND DATES COVERED
	January 1997	Final

4. TITLE AND SUBTITLE

Characterization of Jet Flow From a Decaying Wave Blast Simulator

5. FUNDING NUMBERS

PR: 68N522

6. AUTHOR(S)

Schraml, S.J.

7. PERFORMING ORGANIZATION NAME(S) AND ADDRESS(ES)

U.S. Army Research Laboratory
Weapons & Materials Research Directorate
Aberdeen Proving Ground, MD 21010-5066

8. PERFORMING ORGANIZATION REPORT NUMBER

9. SPONSORING/MONITORING AGENCY NAME(S) AND ADDRESS(ES)

U.S. Army Research Laboratory
Weapons & Materials Research Directorate
Aberdeen Proving Ground, MD 21010-5066

10. SPONSORING/MONITORING AGENCY REPORT NUMBER

ARL-TR-1259

11. SUPPLEMENTARY NOTES

12a. DISTRIBUTION/AVAILABILITY STATEMENT

Approved for public release; distribution is unlimited.

12b. DISTRIBUTION CODE

13. ABSTRACT (Maximum 200 words)

A computational study was performed to characterize the time-dependent jet flow exiting the expansion tunnel of the large blast/thermal simulator (LB/TS). The aerodynamic environment produced by the jet flow has been identified as a possible means of testing full scale military equipment in high drag blast events. Two-dimensional (2-D) axisymmetric calculations were used to estimate the peak pressure, velocity, and impulse levels in the jet flow as a function of the initial conditions. Next, a set of 2-D planar symmetry calculations was performed to assess the effect of the ground plane on the flow field and determine the changes in flow parameters as a function of distance from the exit plane. Finally, a set of three-dimensional (3-D) calculations was used to generate a detailed description of the time-dependent flow and to determine its spatial uniformity for vehicle testing. The 3-D calculation simulating the maximum operational limit of the facility resulted in a peak flow velocity of approximately 420 m/s in an event with a duration of approximately 1.2 s.

14. SUBJECT TERMS

blast   fluid dynamics
flow fields   shock tubes

15. NUMBER OF PAGES

50

16. PRICE CODE

17. SECURITY CLASSIFICATION OF REPORT	18. SECURITY CLASSIFICATION OF THIS PAGE	19. SECURITY CLASSIFICATION OF ABSTRACT	20. LIMITATION OF ABSTRACT
Unclassified	Unclassified	Unclassified	

NSN 7540-01-280-5500

Standard Form 298 (Rev. 2-89)
Prescribed by ANSI Std. Z39-18
298-102